and improved both nutritional status and QOL. Improvement in the sensory properties of food, including appearance, is a simple and nontoxic strategy to increase appetite and QOL in patients with advanced cancer suffering from a loss of appetite.

Loss of appetite is frequently associated with advanced cancer and its treatment. Multiple, interactive factors that are the probable cause of loss of appetite include direct interference of tumors with food intake, malabsorption and poor digestion, and treatment-related complications such as changes in smell and taste. No effective therapy has been established previously for improvement of anorexia in patients with advanced cancer. A simple nontoxic means to improve anorexia would be most benefical in the supportive management of the cancer patient and also could possibly enhance the effectiveness of other therapeutic measures.

Sensory-specific satiety has an important influence on the amount of food eaten [12]. Invariable foods decrease the pleasure of eating even though the food are savory [13-16]. The same phenomenon occurs when eating a sweet food to satiety [13-15] or when drinking a weak-smelling tea compared to a strong-smelling tea [17]. On the other hand, varying the texture of the yogurt in the diet caused a 12.6% elevation of intake compared to the amount of the previously preferred yogurt eaten [14]. Taste, smell, and texture-sepcific satieties are important for regulation of appetite.

Appearance of food is also an important factor involved in sensory-specific satiety. Cancer increases energy expenditure and patients with cancer are normally prescribed a high-calorie diet with heavy appearance of food. In fact, our patient was prescribed a diet of 2000 or 1500 kcal/day, but achieved a caloric intake of only about 600 kcal/day. Since there was no obvious reason for loss of appetite, we assumed that heavy appearance of food spoiled her appetite. Although she was in a state of malnutrition, we reduced her diet to 1000 kcal/day in order to improve appearance of food. In results, the patient's appetite was significantly increased. One would think that chemotherapy itself increased appetite through improvement in cachexia, however, she complained of persistent appetite loss after tumors showed partial remission. On the other hand, Marcelino et al. [18] reported that the desire to eat pizza depended on the visual quality of the pizza. Appearance-specific satiety is also related to areas of the brain that control motivation and the reward value of foods [19-21]. These reports suggests appearance-specific satiety stimulated appetite in our case.

Long-term effects of appearance-specific satiety on the patient's nutritional status was evaluated by measureing total lymphocyte count, an indicator of visceral proteins, and serum albumin levels. We must be cautious in the interpretation of these results because there was no time-couse study in lymphocyte count and albumin levels. Alhough total lymphocyte count did not change, serum albumin levels were significantly increased. The discrepancy between total lymphocyte count and serum albumin levels may be due to adverse effects of chemotherapy. Bone marrow suppression is observed during the chemotherapy which is same regimen used in this case [22] and total lymphocyte count might not reflect the nutritional status adequately in our case. Serum albumin level is a standard marker for evaluation of nutritional status and is not influenced by anti-cancer drug itself. Since serum albumin levels were significantly increased, it is possible that appearance-specific satiety improved long-term status of nutrition in our case.

Appearance-specific satiety increased the scores of SF, ME, RE, and VT of the SF-36 score, which is widely used for evaluating QOL [23,24]. Although it was not clear how appearance-specific satiety increased QOL, following possibilities are exist. Increase in appetite improved the nutritional status. Nutritional status is closely related to liveliness, therefore, improvement of nutritional status may increase in lively aspect of QOL, such as VT. Alternatively, the patient could eat prescribed whole diet by changing the appearance of diet. Eating whole diet was an important achievement and it gave her great pleasure that caused an increase in mental aspects of QOL, such as MH, RE, and SF. Thus, appearance-specific satiety may increase QOL by improvement of lively and mental aspects in our case.

In conclusion, we report here a case in which appearance-specific satiety increased appetite and improved both nutritional status and QOL in patient with advanced cancer. Arrangement for the appearance of food in a diet may be a simple and nontoxic therapeutic strategy for patients who suffered from loss of appetite.

REFERENCES

1. Capra S, Ferguson M, and Ried K. Cancer: impact of nutrition intervention outcome--nutrition issues for patients. Nutrition 2001; 17:769-772.

2. Ottery FD. Cancer cachexia: prevention, early diagnosis, and management. Cancer Pract 1994; 2:123-131.
3. Corli O, Cozzolino A, Battaiotto L, Bernoni M, and Gallina A. A new method of food intake quantification: application to the care of cancer patients. J Pain Symptom Manage 1992; 7:12-17.
4. Rivadeneira DE, Evoy D, Fahey TJ 3rd, Lieberman MD, and Daly JM. Nutritional support of the cancer patient. CA Cancer J Clin 1998; 48:69-80.
5. Shils ME. Principles of nutritional therapy. Cancer 1979; 43:2093-2102.
6. Bruera E. Pharmacological treatment of cachexia: any progress? Support Care Cancer 1998; 6:109-113.
7. Bruera E, Belzile M, Neumann C, Harsanyi Z, Babul N et al. A double-blind, crossover study of controlled-release metoclopramide and placebo for the chronic nausea and dyspepsia of advanced cancer. J Pain Symptom Manage 2000; 19:427-435.
8. Rolls BJ, Rowe EA, and Rolls ET. How sensory properties of foods affect human feeding behavior. Physiol Behav 1982; 29:409-417.
9. Sorensen LB, Moller P, Flint A, Martens M, and Raben A. Effect of sensory perception of foods on appetite and food intake: a review of studies on humans. Int J Obes Relat Metab Disord 2003; 27:1152-1166.
10. Kawaguchi T, Tanaka M, Itano S, Ono N, Shimauchi Y et al. Successful treatment for bronchial bleeding from invasive pulmonary metastasis of hepatocellular carcinoma: a case report. Hepatogastroenterology 2001; 48:851-853.
11. Keys A. Energy requirements of adults. J Am Med Assoc 1950; 142:333-338.
12. Rolls BJ, Rolls ET, Rowe EA, and Sweeney K. Sensory specific satiety in man. Physiol Behav 1981; 27:137-142.
13. Guinard JX, and Brun P. Sensory-specific satiety: comparison of taste and texture effects. Appetite 1998; 31:141-157.
14. Rolls BJ, Rowe EA, Rolls ET, Kingston B, Megson A et al. Variety in a meal enhances food intake in man. Physiol Behav 1981; 26:215-221.
15. Rolls BJ, Van Duijvenvoorde PM, and Rolls ET. Pleasantness changes and food intake in a varied four-course meal. Appetite 1984; 5:337-348.
16. Rolls ET, Rolls BJ, and Rowe EA. Sensory-specific and motivation-specific satiety for the sight and taste of food and water in man. Physiol Behav 1983; 30:185-192.
17. Vickers Z, and Holton E. A comparison of taste test ratings, repeated consumption, and postconsumptin ratings of different strengths of iced tea. J Sensory Stud 1998; 13:199-212.
18. Marcelino AS, Adam AS, Couronne T, Koster EP, and Sieffermann JM. Internal and external determinants of eating initiation in humans. Appetite 2001; 36:9-14.
19. O'Doherty J, Rolls ET, Francis S, Bowtell R, McGlone F et al. Sensory-specific satiety-related olfactory activation of the human orbitofrontal cortex. Neuroreport 2000; 11:399-403.
20. Rolls ET. The neurophysiology of feeding. Int J Obes 1984; 8 (Suppl 1):139-150.
21. Yaxley S, Rolls ET, Sienkiewicz ZJ, and Scott TR. Satiety does not affect gustatory activity in the nucleus of the solitary tract of the alert monkey. Brain Res 1985; 347:85-93.
22. Anami Y, Oguma S, Matsuda Y, Yamaki T, Sazawa Y et al. Complete disappearance of metastatic lung tumors and mediastinal lymphnode in a case of hepatocellular carcinoma treated by low-dose 5-fluorouracil/cisplatin therapy. Gan To Kagaku Ryoho 2005; 32:1977-1980. (in Japanese)
23. Fukuhara S, Bito S, Green J, Hsiao A, and Kurokawa K. Translation, adaptation, and validation of the SF-36 Health Survey for use in Japan. J Clin Epidemiol 1998; 51:1037-1044.
24. Ware JE Jr., and Sherbourne CD. The MOS 36-item short-form health survey (SF-36). I. Conceptual framework and item selection. Med Care 1992; 30:473-483.

Digestive Diseases and Sciences, Vol. 51, No. 6 (June 2006), pp. 1057–1060 (© 2006)
DOI: 10.1007/s10620-006-8008-9

Branched-Chain Amino Acid Supplementation Complements Conventional Treatment for Spontaneous Bacterial Peritonitis

EITARO TANIGUCHI, MD, PhD,† TAKUMI KAWAGUCHI, MD, PhD,* MARI SHIMADA, MD,† REIICHIRO KUWAHARA, MD, PhD,† YUMIKO NAGAO, MD, DDS,* MOMOKA OTSUKA, Dietitian,† SHOKO IWASAKI, Dietitian,† TOKIKO MATSUDA, Nrs,† RYOKO IBI, Nrs,† SATOMI SHIRAISHI, Nrs,† MINORU ITOU, MD,† TETSUHARU ORIISHI, MD,† RYUKICHI KUMASHIRO, MD, PhD,† SHOKO TANAKA, Dietitian,† YUKO SARUWATARI, Nrs,† and MICHIO SATA, MD*

KEY WORDS: nutrition; liver failure; late evening snack; hepatic fibrosis; hepatocyte growth factor.

Spontaneous bacterial peritonitis (SBP) is a life-threatening complication of liver cirrhosis (1). The prevalence of SBP among hospitalized cirrhotic patients with ascites has been estimated to be approximately 15% (2). SBP in cirrhotic patients is thought to occur as a consequence of impaired defensive mechanisms against infection, such as a decrease in the lymphocyte count and an impaired phagocytic function of neutrophils (3).

Mortality rate related to SBP has been improved by the development of new antibiotics (4); however, the rate is still 17–50% (2). Branched-chain amino acids (BCAA) supplementation improves not only the nutritional and metabolic status such as serum albumin concentration and Fisher's ratio, but also defensive mechanisms against infection in cirrhotic patients (5). Strengthening of resistance to infection is believed to be the result of the elevation of the absolute lymphocyte count (6). Moreover, a recent study disclosed that BCAA supplementation improves phagocytic function of neutrophils in cirrhotic patients (7). Although BCAA supplementation seems to be an effective therapy in patients with SBP, the beneficial effects of BCAA supplementation have never been reported in this regard.

In this report, we present the first documented case showing that BCAA supplementation complements conventional treatment for SBP and subsequent liver failure. BCAA supplementation should be considered as a complementary treatment for patients with SBP.

Manuscript received January 24, 2005; accepted July 12, 2005.

From the *Department of Digestive Disease Information and Research and †Nutritional Curative Team and Second Department of Medicine, Kurume University School of Medicine, Kurume, Japan.

Address for reprint requests: Eitaro Taniguchi, MD, PhD, Second Department of Medicine, Kurume University School of Medicine, 67 Asahi-machi, Kurume 830-0011, Japan; eitaro@med.kurume-u.ac.jp.

CASE REPORT

A 71-year-old Japanese woman was referred to Kurume University Hospital for abdominal pain. Chronic hepatitis C was diagnosed when the patient was 54 years old. Despite various treatments including interferon, liver cirrhosis developed when the patient was 66 years old. Ascites was evident 2 months before the patient presented with abdominal pain.

Physical examination showed a height of 152 cm and a weight of 51.7 kg. Vital signs were within normal range except for her body temperature (BT) of 37.2 °C. The patient had icteric pigmentation of the sclera and skin, tense ascites, and peripheral edema. Laboratory data on admission are summarized in Table 1. Briefly, liver failure with inflammation was indicated. In the patient's ascitic fluid, the protein concentration was 0.29 g/dL and the polymorphonuclear count was 837/mm^3; few red blood cells and no malignant cells were seen. Abdominal x-ray showed no free air. Abdominal ultrasound examination showed no findings suggesting acute pancreatitis, tumor, or hemorrhage in the abdominal organs. Although no pathogenic organisms could be isolated from the ascites or peripheral blood, the patient exhibited abdominal pain and fever, a polymorphonuclear count >500/mm^3 in the ascitic fluid, and an absence of clinical, laboratory, radiologic, and ultrasound findings suggesting secondary peritonitis. Therefore, a diagnosis of SBP with liver failure was established.

SBP was immediately treated with a third-generation cephalosporin (sulbactam/cefoperaazone; Figure 1). Infusions of albumin were also administered to reduce the risk of renal failure and disseminated intravascular coagulation. At first, the antibiotic treatment seemed to be effective because the serum CRP concentration gradually decreased; however, the patient exhibited persistent fever and abdominal pain. The antibiotic was then

TABLE 1. LABORATORY DATA ON ADMISSION

Hematology		Glucose	84 mg/dL
WBC	5,600/mm^3	BUN	21.7 mg/dL
Neutrocytes	68.5%	Creatinine	0.66 mg/dL
Lymphocytes	23.5%	Na^+	143 mEq/L
RBC	361 x 10^4 mm^3	K^+	4.5 mEq/L
Platelets	3.4 x 10^4 mm^3	Cl^-	107 mEq/L
Biochemical examination		Prothrombin time	55%
AST	142 U/L	Endotoxin	<0.4 pg/mL
ALT	132 U/L	Blood culture	negative
LDH	494 U/L	**Ascitic fluid examination**	
Total protein	5.54 g/dL	Gross appearance	turbid
Albumin	2.7 g/dL	Protein	0.29 g/dL
Total bilirubin	3.74 mg/dL	WBC	1922/ mm^3
Direct bilirubin	1.10 mg/dL	Polymorphonuclear cells	837/ mm^3
CRP	7.15 mg/dL	culture	negative

changed to a carbapenem (imipenem/cilastatin) and infusions of γ-globulin were also administered. To improve the patient's nutritional status and resistance to infection, 50 g of Aminoleban EN containing abundant BCAA with 210 kcal energy (Table 2) was given as a late evening snack, although no findings of hepatic encephalopathy were seen. We also treated a decayed tooth, because it could have been an origin for elevated CRP concentration. With these treatments, abdominal pain disappeared, and BT and serum CRP concentration gradually decreased. However, BT and CRP concentration were not fully normalized, and a subsequent increase in serum total bilirubin concentration and a decrease in prothrombin activity occurred, indicating development of severe liver failure.

The patient's required energy expenditure was estimated to be 1700–1842 kcal/d based on the Harris-Benedict formula (8). Although the patient seemed to have an adequate dietary caloric intake with the BCAA supplementation, the serum concentration of free fatty acids showed 1531 μEq/L (normal range,

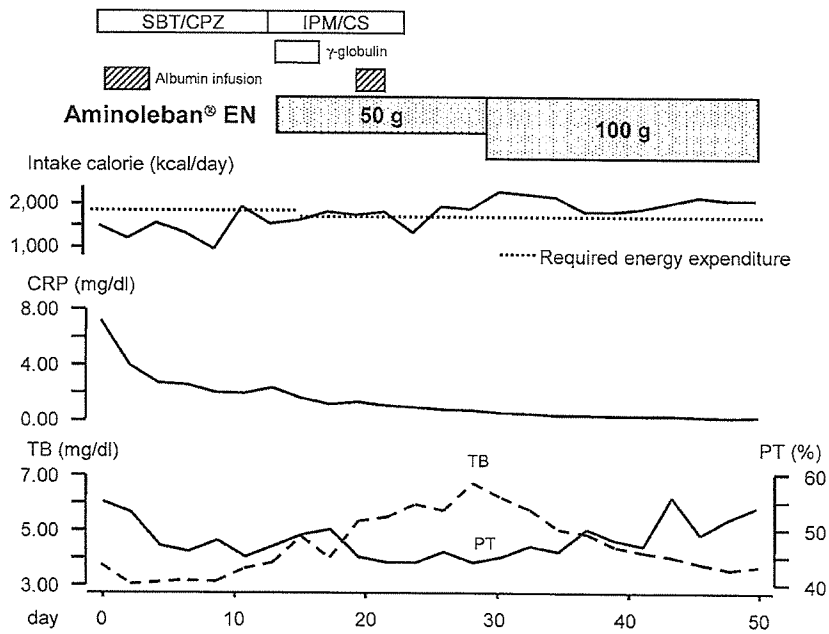

Fig 1. Laboratory indices over the days of admission. By treatment with antibiotics and γ-globulin infusions, CRP concentration gradually decreased. However, CRP concentration was not fully normalized. Total bilirubin reachd peak value and prothrombin activity reached its nadir on day 29. There was a dramatic response to additional administration of BCAA supplementation (total 100 g), with decrease in total bilirubin concentration and increase in prothrombin activity. CRP concentration returned to normal. *Abbreviations:* SBT/CPZ, sulbactam/cefoperazone; IPM/CS, imipenem/cilastatin; TB, total bilirubin; PT, prothrombin activity.

TABLE 2. COMPOSITION OF AMINOLEBAN EN (PER 50 G)

Total energy	210 kcal	Histidine	0.27 g
Protein	13.5 g	Proline	0.98 g
Amino acids		Serine	0.24 g
(Fischer's ratio = 38)			
Valine	1.79 g	Tyrosine	0.05 g
Leucine	2.25 g	Lysine	0.60 g
Isoleucine	2.04 g	Aspartic acid	0.45 g
Threonine	0.29 g	Glutamic acid	0.85 g
Tryptophan	0.08 g	Glycine	1.74 g
Methionine	0.06 g	Fat (rice oil)	3.50 g
Phenylalanine	0.17 g	Carbohydrates (Dextrin)	31.05 g
Alanine	0.75 g	Vitamins	
Arginine	0.88 g	Minerals	

Note. Vitamins include trace amounts of magnesium sulphate, calcium glycerophosphate, potassium iodide, potassium chloride, sodium dihydrogen phosphate dihydrate, sodium ferrous citrate, cupric sulphate, zinc sulphate, and manganese sulphate. Minerals include retinol palmitate, ergocalciferol, bisbentiamine, riboflavin, pyridoxine HCl, cyanocobalamin, folic acid, sodium l-ascorbate, tocopherol acetate, phytonadione, calcium pantothenate, nicotinamide, and biotin.

100–540 μEq/L), suggesting starvation. Moreover prothrombin activity was only 44% of normal, indicating impaired protein synthesis. We therefore administered additional BCAA supplementation after breakfast to improve the protein–energy malnutrition condition.

This action resulted in a dramatic decrease of total bilirubin concentration and increased prothrombin activity as well as the disappearance of ascites and peripheral edema (see Figure 1). Moreover, BT and CRP concentration were normalized with BCAA supplementation without the use of antibiotics. Simultaneously, increases in total lymphocyte count and serum hepatocyte growth factor (HGF) concentration were seen (Figure 2). Thus, SBP and subsequent liver failure were successfully managed.

We continued the BCAA supplementation. At 3 months' follow-up, the patient did not show any evidence of SBP or liver failure, and the serum concentrations of hyaluronic acid and type IV collagen were decreased, suggesting improvement of hepatic fibrosis (Figure 3).

DISCUSSION

This represent the first description of a case showing BCAA supplementation complementing conventional treatment of SBP. Thus, the use of BCAA supplementation as add-on therapy to antibiotics appears to reduce the risk of mortality in patients with SBP.

Although recent advances in the diagnosis and treatment of bacterial infections have improved the prognosis in patients with SBP (9), SBP accompanying severe liver failure continues to have a poor prognosis. Tito *et al.* reported that predictive factors for poor prognosis of SBP patients were serum bilirubin >4 mg/dL, prothrombin activity ≤45%, and protein concentration in ascitic fluid ≤1 g/dL (1). The patient in the current report demonstrated even poorer values for all of the predictive factors; therefore, poor prognosis was anticipated.

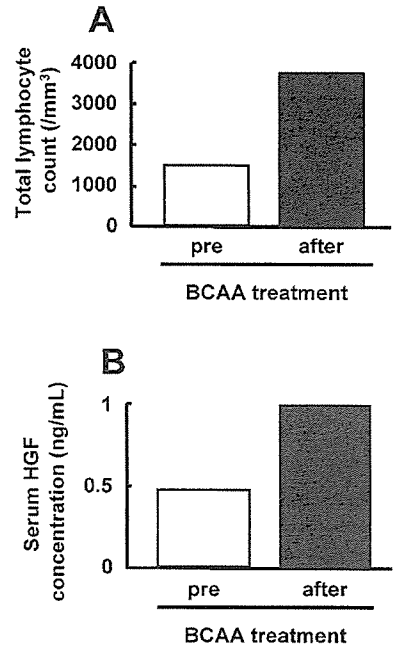

Fig 2. The effects of BCAA supplementation on total lymphocyte count (A) and serum HGF concentration (B). Total lymphocyte count and serum HGF concentration were increased by administration of BCAA supplementation.

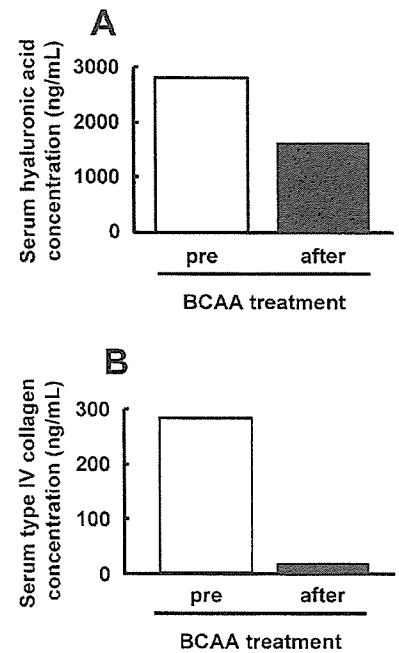

Fig 3. The effects of BCAA supplementation on serum concentrations of hyaluronic acid (A) and type IV collagen (B). Serum concentrations of hyaluronic acid and type IV collagen were decreased by administration of BCAA over 3 months.

After the administration of antibiotics and BCAA supplementation in our patient, abdominal pain disappeared and BT and CRP concentration normalized. Carbapenem and γ-globulin played a significant role in suppression of the bacterial infection; however, BT and CRP concentration did not revert to the normal range. BCAA administration has been shown to improve immune function parameters, for example, the elevation of total lymphocyte count (6). In our patient, total lymphocyte count was increased from 1450–3740/μL. Furthermore, BCAA supplementation is reported to improve phagocytic function of neutrophils in cirrhotic patients (7). Taken together, these observations indicate that BCAA supplementation the the potential to complement conventional treatment for patients with SBP.

Given a similar situation as that of our patient, one would most likely choose total parenteral nutrition rather than enteral nutrition. However, additional bacterial translocation may occurr because the defensive mechanisms of gut against infection are weakened. This suggests that total parenteral nutrition may worsen the prognosis for patients with SBP. Therefore, it is recommended that these patients be treated via enteral nutrition.

Because our patient appeared to suffer from both of starvation and protein synthesis, additional BCAA supplementation was given to improve protein–energy malnutrition. The administration of additional BCAA supplementation caused a dramatic decrease of total bilirubin concentration and an increase in prothrombin activity. BCAA supplementation has been reported to have various pharmacologic effects besides being an essential substrate for protein synthesis. Tomiya *et al.* reported that BCAA, especially leucine, stimulate the production of HGF by hepatic stellate cells (10). HGF stimulates proliferation of hepatocytes and bile duct epithelial cells (10) and facilitates liver regeneration. Moreover, HGF prevents hepatic fibrogenesis. Therefore, a possible explanation for the recovery from severe liver failure is that BCAA supplementation leads to an increase in HGF production by hepatic stellate cells and subsequently improves liver failure through promotion of liver regeneration and inhibition of fibrogenesis. This possibility is supported by observations in our patient: serum HGF concentration was increased after administration of BCAA supplementation and serum hyaluronic acid and type IV collagen concentrations, both indicators of hepatic fibrosis, were decreased.

In conclusion, we report a case herein, where BCAA supplementation complemented conventional treatment for SBP and subsequent liver failure. BCAA supplementation should be considered as complementary therapy for patients with SBP.

ACKNOWLEDGMENTS

Supported in part by a grant from the Ishibashi Foundation for the Promotion of Science and a Grant-in-Aid for Scientific Research (C) (No. 15590963 to T.K., No. 16590648 to M.S.) and for Young Scientific Research (B) (No. 14770260 to E.T.) from the Ministry of Education, Culture, Sports, Science and Technology of Japan.

REFERENCES

1. Tito L, Rimola A, Gines P, Llach J, Arroyo V, Rodes J: Recurrence of spontaneous bacterial peritonitis in cirrhosis: frequency and predictive factors. Hepatology 8:27–31, 1988
2. Hoefs JC: Spontaneous bacterial peritonitis: prevention and therapy. Hepatology 12:776–781, 1990
3. Crossley IR, Williams R: Spontaneous bacterial peritonitis. Gut 26:325–331, 1985
4. Taskiran B, Colakoglu O, Sozmen B, Unsal B, Aslan SL, Buyrac Z: Comparison of cefotaxime and ofloxacin in treatment of spontaneous bacterial peritonitis. Turk J Gastroenterol 15:34–38, 2004
5. Habu D, Nishiguchi S, Nakatani S, *et al.*: Effect of oral supplementation with branched-chain amino acid granules on serum albumin level in the early stage of cirrhosis: a randomized pilot trial. Hepatol Res 25:312–318, 2003
6. Cerra FB, Mazuski JE, Chute E, *et al.*: Branched chain metabolic support. A prospective, randomized, double-blind trial in surgical stress. Ann Surg 199:286–291, 1984
7. Nakamura I, Ochiai K, Imawari M: Phagocytic function of neutrophils of patients with decompensated liver cirrhosis is restored by oral supplementation of branched-chain amino acids. Hepatol Res 29:207–211, 2004
8. Long CL, Schaffel N, Geiger JW, Schiller WR, Blakemore WS: Metabolic response to injury and illness: estimation of energy and protein needs from indirect calorimetry and nitrogen balance. JPEN J Parenter Enteral Nutr 3:452–456, 1979
9. Garcia-Tsao G: Bacterial infections in cirrhosis. Can J Gastroenterol 18:405–406, 2004
10. Tomiya T, Omata M, Fujiwara K: Significance of branched chain amino acids as possible stimulators of hepatocyte growth factor. Biochem Biophys Res Commun 313:411–416, 2004

Antibody to hepatitis B core antigen is associated with the development of hepatocellular carcinoma in hepatitis C virus-infected persons: A 12-year prospective study

KAZUO TANAKA[1], YUMIKO NAGAO[1,2], TATSUYA IDE[1,2], RYUKICHI KUMASHIRO[1] and MICHIO SATA[1,2]

[1]Second Department of Medicine and [2]Department of Digestive Disease Information and Research, Kurume University School of Medicine, Asahi-machi, Kurume, Fukuoka 830-0011, Japan

Received December 9, 2005; Accepted January 26, 2006

Abstract. Several studies have reported that antibody to hepatitis B core antigen (anti-HBc) positivity may influence the development of hepatocellular carcinoma (HCC) in chronic hepatitis C patients, but the evidence is still not conclusive. In this study, we examined whether the presence of anti-HBc positive was associated with the development of HCC in hepatitis C virus (HCV)-infected subjects among the residents in an HCV hyperepidemic area who were followed up for 12 years. In an HCV hyperendemic area (positive rate of anti-HCV: 23.4%), 509 residents were examined by health screening in 1990. After 12 years of follow-up, we evaluated the risk factors for HCC. The incidence of HCC was compared between anti-HBc positive and anti-HBc negative subjects after 12 years of prospective observation. Univariate and multivariate analyses were conducted to determine risk factors for the development of HCC. The incidence of HCC was significantly higher in the anti-HBc positive group (13 subjects) than in the anti-HBc negative group (0 subjects) (P=0.012). Multivariate analysis identified positivity for anti-HBc and HCV RNA, history of icterus, and female gender as independent determinants of the development of HCC. Our findings provide clear evidence in a prospective study that presence of anti-HBc, that is, past hepatitis B virus (HBV) infection, is a risk factor for the development of HCC in HCV-infected people.

Introduction

The number of hepatitis B virus (HBV) and hepatitis C virus (HCV) infection carriers worldwide is estimated at 350 million (1) and 170 million (2), respectively. HBV and HCV infections include substantial proportions of cases with past infection, asymptomatic carriers, acute hepatitis and chronic hepatitis, and HBV infections may cause fulminant hepatitis. Especially, chronic HBV and HCV infections may lead to cirrhosis and hepatocellular carcinoma (HCC) (1,3). It was reported that the frequency of HCC due to chronic HCV infection is higher in Japan than in any other country (4). Several studies have reported that occult HBV infection may also be one of the causative factors of HCC (5,6). The presence of occult HBV infection is diagnosed based on the fact that HBV DNA still exists in serum and liver tissue after hepatitis B surface antigen (HBsAg) disappears in acute or chronic HBV infection (7-9), or even after antiviral treatment is successful. Although some studies reported that occult HBV infection is associated with HCV-related liver dysfunction (10) or the development of HCC (11-13), these associations have still not been clearly demonstrated in a prospective study.

A higher incidence of HBV DNA is commonly seen in patients with anti-HBc-positive serology than in those with anti-HBc negative serology in coinfections with HBV and HCV (10), and using PCR amplification, most studies have demonstrated the presence of the HBV DNA genome in 22% to 87% of the patients who are HBsAg negative and HCV RNA positive (10,14-18). Some studies showed that HBV infection could occur in recipients of livers donated from subjects with anti-HBc but without HBsAg (19,20). That is, anti-HBc, which was initially considered to be an index for the past HBV infection in which all HBV had been cleared, has emerged as a convincing marker of occult hepatitis B (19,21-23). Also, several studies showed that the anti-HBc positivity was associated with the development of HCC in patients with HCV-associated chronic liver disease (11,24-26), but these associations have not been clearly demonstrated.

Since 1990, we have conducted health screenings of the residents of H town (adult population: 7,389), Fukuoka prefecture in northern Kyushu, Japan (27). This town is known for its high prevalence of liver disease. We previously reported that the town had a high prevalence of HCV carriers, 120/509 (23.6%) in 1990, and that HCV infection was the principal cause of liver dysfunction and HCC (27,28).

In the present study, we analyzed the influence of anti-HBc positivity on the development of HCC in HCV-infected people in the same town during 12 years in a prospective manner.

Correspondence to: Dr Kazuo Tanaka, Second Department of Internal Medicine, Kurume University School of Medicine, 67 Asahimachi, Kurume 830-0011, Japan
E-mail: wada.isi@alto.ocn.ne.jp

Key words: antibody to hepatitis B core antigen, occult hepatitis B virus, hepatitis C virus, hepatocellular carcinoma, HCV hyper epidemic area

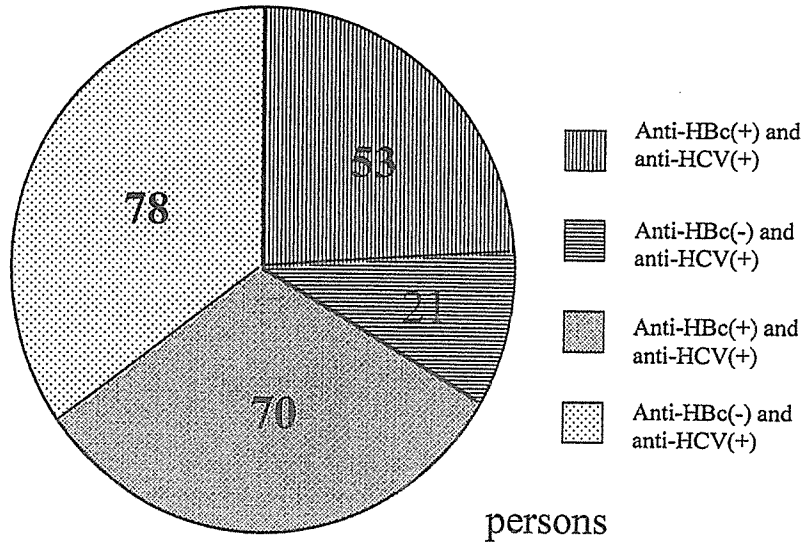

Figure 1. Diagram showing incident of hepatitis virus markers (anti-HCV and anti-HBc) among the 222 inhabitants 12 years ago. Fifty-three inhabitants were anti-HBc positive and anti-HCVpositive, 21 were anti-HBc negative and anti-HCVpositive, 70 were anti-HBc positive and anti-HCV negative, and 78 were anti-HBc negative and anti-HCV negative.

Subjects and methods

Subjects. In 1990, of a total 9,799 inhabitants, 739 (10%) of the 7,389 inhabitants >20 years old were randomly selected as follows: the names of the residents (as they appeared on their resident cards) were arranged in order according to the Japanese phonetic syllabary. Then every tenth resident was selected. As a result, 509 subjects (6.9% of H town residents) gave their informed consent to participate in the study.

Of 509 participants initially screened in 1990, 69 people had died and 55 people had moved to other regions as of 2002. Thus, 385 of the original 509 residents survived in the area and 139 residents agreed to participate in the medical follow-up survey, while 26 did not agree to participate, and the remaining 220 residents did not declare their intention either way in 2002. For 14 of these remaining 220 inhabitants, the records were obtained from the primary physicians. Consequently, we analyzed the outcome in terms of the liver disease in 222 inhabitants (69+139+14) in 2002.

Information on cigarette smoking, alcohol consumption, and history of icterus, and blood transfusion was obtained at the time of enrollment through interviews by the doctors in charge and experienced public health nurses. Smoking was defined as >10 cigarettes per day for >10 years. Alcohol consumption was defined as a daily intake of ≥75 g of ethanol per day for >10 years.

Serological assay. In 1990, sera were collected from all the participants, and conventional liver function tests were performed: serum levels of aspartate aminotransferase (AST), alanine aminotransferase (ALT), gammaglutamyl transpeptidase (γ-GTP), total protein (TP), albumin (Alb), total cholesterol (TC), total bilirubin (TB), zinc turbidity (ZTT) were measured. Anti-HCV was measured using HCV PHA 2nd generation kits (Dainabot Co. Ltd., Tokyo, Japan). These results were confirmed using a second generation recombinant immunoblot assay (RIBA II) (Ortho Diagnostic System, Tokyo, Japan). Measurement of HBsAg and anti-HBc was performed with an enzyme immunoassay kit (Mizuho Medy Co. Ltd., Tosu, Saga, Japan). Titers of anti-HBc yielding >70% inhibition were assessed as positive.

Detection of HCV RNA by RT-PCR. All subjects who were anti-HCV-positive were tested for the presence of serum HCV RNA, which was detected by reverse transcription-nested polymerase chain reaction (RT-nested PCR) using primers based on the sequences of the 5'UTR (untranslated region) of the HCV genome, as described previously (29).

Statistical analysis. Continuous data were expressed as mean ± SD, minimum and maximum. Categorical data were expressed as frequency and/or percentage. For comparing the background between anti-HBc positive and negative, the χ^2 and Wilcoxon's test were used to analyze quantitative data. Univariate and multivariate analysis were performed by logistic regression to calculate odds ratio and its 95% confidence interval. The SAS (statistical analysis system) computer program (release 8.2; SAS Institute Inc., Cary, NC, USA) was used for the logistic regression. A P-value of <0.05 was considered statistically significant.

Results

In 2002, anti-HCV was detected in 74 of the 222 inhabitants (Fig. 1). HCV RNA was detected in 53 (71.6%), HBsAg in 1 (1.4%), and anti-HBc in 53 (71.6%) of these 74 people. We asked the primary physician of these 74 inhabitants about the diagnosis of liver disease, and found thereby that 8 inhabitants had died of HCC and 5 inhabitants had been treated for HCC (total 13 inhabitants).

The 74 inhabitants were divided into two groups: 53 who were positive and 21 who were negative for anti-HBc, and the clinical characteristics observed in the screening were compared between the two groups. No significant differences

Table I. Characteristics of anti-HCV positive patients with and without anti-HBc.

Characteristics	Anti-HBc positive (N=53)	Anti-HBc negative (N=21)	P-value
Age (year)	62.3±10.9	58.0±16.4	NS
Sex: M:F	23:30	05:16	NS
Smoking (%)	16 (30.2)	4 (19.0)	NS
History of icterus (%)	8 (15.1)	3 (14.3)	NS
Alcohol consumption (%)	3 (5.7)	2 (9.5)	NS
History of blood transfusion (%)	8 (15.1)	4 (19.0)	NS
ALT level (IU/l)	40.6±30.8	27.5±17.9	NS
HBsAg (%)	1 (1.9)	0 (0)	NS
HCV RNA (%)	39 (73.6)	14 (66.7)	NS
HCC (%)	13 (24.5)	0 (0)	0.012

Age and serum ALT level were expressed as mean ± SD. HCC, hepatocellular carcinoma; NS, not significant.

Table II. Univariate analysis of risk factors that influence the development of HCC.

Factors	HCC group (n=13)	non-HCC group (n=61)	Odds ratio	95% CI	P-value
Age (years)	65.3±8.1 (53-82)	60.1±13.4 (23-89)	1.035	0.984-1.088	0.1866
Sex: male (%)	6 (46.2)	22 (36.1)	0.658	0.196-2.205	0.4976
Smoking (%)	4 (30.8)	13 (21.3)	1.641	0.435-6.190	0.4646
Alcohol consumption (%)	5 (38.5)	22 (36.1)	1.108	0.323-3.804	0.8706
History of blood transfusion (%)	3 (23.1)	8 (13.1)	1.988	0.448-8.810	0.3659
History of icterus (%)	5 (38.5)	5 (8.2)	7.000	1.652-29.667	0.0083[a]
AST (IU/l)	65.5±31.1 (28-131)	33.0±21.9 (13-132)	1.041	1.015-1.068	0.0016[a]
ALT (IU/l)	57.5±24.8 (20-108)	32.6±27.1 (9-160)	1.028	1.006-1.050	0.0119[a]
γ-GTP (IU/l)	127.1±195.3 (17-720)	32.4±34.2 (7-196)	1.015	1.003-1.027	0.0158[a]
Total protein (IU/l)	7.97±0.88 (6.6-10.0)	8.05±0.58 (6.6-9.8)	0.808	0.309-2.107	0.6622
Albumin (g/dl)	3.98±0.49 (3.0-4.9)	4.33±0.31 (3.2-4.8)	0.094	0.017-0.507	0.0060[a]
Total cholesterol (mg/dl)	160.5±33.1 (111-224)	173.8±32.5 (111-257)	0.987	0.967-1.007	0.1851
Total bilirubin (mg/dl)	1.01±0.50 (0.5-2.3)	0.77±0.27 (0.4-1.3)	7.537	1.170-48.533	0.0335[a]
ZTT (KU)	15.35±5.76 (1.1-21.7)	11.40±4.86 (2.5-27.4)	1.161	1.026-1.314	0.0183[a]
Anti-HBc (%)	13 (100)	40 (65.6)	9.150	1.407-	0.0161[a]
HCV RNA (%)	13 (100)	40 (65.6)	9.150	1.407-	0.0161[a]

[a]P<0.05; HCC, hepatocellular carcinoma; CI, confidence interval. Age, AST, ALT, γ-GTP, total protein, albumin, total bilirubin and ZTT were expressed as mean ± SD (range).

were observed between the two groups in age, sex, smoking, history of icterus or blood transfusion, alcohol consumption, ALT level, HBsAg, or HCV RNA. Significant differences were observed for the incidence of HCC (13 versus 0) between these two groups (P=0.012) (Table I).

Univariate and multivariate analyses of factors that influenced the incidence of HCC. The influence of age, sex, smoking, history of icterus, history of blood transfusion, alcohol consumption, AST, ALT, γ-GTP, TP, Alb, TC, TB, ZTT, anti-HBc and HCV RNA on the development of HCC was analyzed by univariate and multivariate analyses.

Table II shows the basic characteristics of the 74 inhabitants with anti-HCV divided into two groups: a group with HCC (HCC group) and a non-HCC group, and shows the results of univariate analyses. The mean age and sex were not significantly different between the HCC group and non-HCC group. Serum levels of AST, ALT, γ-GTP, TB, and ZTT were significantly higher in the HCC group than in the non-HCC group (P<0.05). The serum level of Alb was significantly lower in the HCC group than in the non-HCC group (P<0.05). The frequency of anti-HBc, HCV RNA, and history of icterus were significantly higher in the HCC group than in the non-HCC group (P<0.05). The frequency of smoking, alcohol

Table III. Multivariate analysis of risk factors that influence the development of HCC.

Factors	Odds ratio	95% CI	P-value
Age (years)	0.987	0.852-1.132	0.8428
Sex: female	190.517	2.157- >999.999	0.0188[a]
Smoking	40.580	0.656- >999.999	0.0824
Alcohol consumption	5.051	0.163-3.804	0.3644
History of blood transfusion	0.964	<0.001- >999.999	0.9918
History of icterus	311.186	5.066- >999.999	0.0042[a]
AST (IU/l)	1.013	0.855-1.244	0.8776
ALT (IU/l)	0.974	0.791-1.101	0.7013
γ-GTP (IU/l)	1.006	0.990-1.080	0.6950
Total protein (IU/l)	15.131	0.227- >999.999	0.2035
Albumin (g/dl)	<0.001	<0.001-11.319	0.1236
Total cholesterol (mg/dl)	1.018	0.952-1.106	0.6028
Total bilirubin (mg/dl)	7.911	0.060- >999.999	0.4127
ZTT (KU)	0.695	0.370-1.196	0.1853
Anti-HBc positive	>999.999	1.556-	0.0292[a]
HCV RNA positive	>999.999	3.767-	0.0063[a]

[a]P<0.05; HCC, hepatocellular carcinoma; CI, confidence interval.

consumption, and history of blood transfusion were not significantly different between the HCC group and non-HCC group.

Multivariate logistic regression analyses identified anti-HBc positivity, HCV RNA positivity, history of icterus, and female sex as independent risk factors for the development of HCC (Table III).

Discussion

Several studies have shown that anti-HBc positivity was associated with the development of HCC in patients with HCV-associated chronic liver disease (11,24-26). However, considering the natural history of all HCV infections, the results of those previous studies have some problems, i.e., the observation period was short and the research was performed in a retrospective manner in patients with chronic hepatitis and liver cirrhosis. Our study was a prospective study that investigated the disease progress after 12 years, and was thought to reflect the natural history of HCV infections, because we did not investigate only HCV-associated chronic liver disease but also covered all HCV infections such as past HCV infection and asymptomatic carriers of HCV (30,31). In this study, we obtained clear evidence that anti-HBc-positivity was a risk factor for the development of HCC in HCV-infected people.

It has been suggested that HBV can induce liver tumor formation by at least two distinct mechanisms. First, HBV DNA sequences are frequently found integrated into chromosomes of hepatocytes that have evolved into HCC, and a direct role of HBV in hepatocarcinogenesis has thus been inferred (32,33). Second, HBV DNA sequences may be caused by disruption of tumor suppressor gene function (34). It has been shown that HBV DNA sequences can be detected in some of the liver or serum from anti-HBc-positive patients (9,10), and the presence of anti-HBc does not entirely exclude the possibility of chronic HBV infection. Though the presence of anti-HBc has been used as a marker of past HBV infection, the integration of HBV DNA in hepatocytes may cause carcinogenesis, as noted above. That is, anti-HBc-positivity may represent occult HBV infection. The presence of anti-HBc alone, in the absence of HBV DNA testing, has been used in some studies as a marker of occult hepatitis B (19,21-23). Pollicino *et al* provided clear evidence that occult HBV was a risk factor for the development of HCC and showed that the potential mechanisms whereby HBV might induce tumor formation occur in most cases of occult infection (6).

To detect occult HBV infection, it is necessary to examine whether HBV DNA is present. However, serum HBV DNA levels are frequently below the limits of detection in anti-HBc-positive patients, and there is a pronounced risk of false-positive results from contamination (35) or amplification of non-HBV-DNA targets, and the sensitivity of detection is variable (36,37). In a previous study in which serum HBV DNA was tested in 20 anti-HBc positive patients with HCV-associated HCC, HBV DNA was not detected by a real-time PCR assay with a minimum detection limit of $10^{1.7}$ copies/ml (1.7 log copies/ml) (38,39). Considering these results, it might not be possible to detect serum HBV DNA in some anti-HBc-positive subjects. Therefore, if we could examine liver tissues by PCR to examine whether occult HBV infection is present, we could be more certain of the presence of occult HBV infection.

In contrast to our findings, in some studies anti-HBc positivity was not found to be associated with the development

of HCC in patients with HCV-associated chronic liver disease (9,39,40). One study showed that anti-HBc was detected significantly more frequently in blood donors with than without anti-HCV, but the prevalence of anti-HBc was no different between the patients with HCV-associated HCC and anti-HCV-positive blood donors. Therefore, no epidemiological evidence was obtained for a role of past HBV infection in hepatocarcinogenesis in patients infected with HCV in Japan (40). Also, Yano *et al* showed that the clinical features of HCV-associated HCC were unaffected by anti-HBc-positivity (39). In addition, a study in Taiwan suggested that occult HBV infection might have little influence on the clinicopathologic course of chronic HCV infection (9).

It was reported that the frequency of HCC due to chronic HCV infection is higher in Japan compared with any other country (4). If the frequency of HCC due to chronic HCV infection is high, it is necessary to consider the possibility that anti-HBc positivity may be associated with hepatocarcinogenesis. In addition to HBV, other environmental and host factors might also be associated with the pathogenesis of HCC (4,41-43).

We continued carrying out health screenings of the residents of H town and conducted a cohort study of liver disease among the same residents over a 12-year period. The results of this study showed that anti-HBc is associated with the development of HCC in HCV-infected people.

Acknowledgements

We would like to thank the following institutions for collection of data of the residents' liver disease: Amagi Asakura Medical Association Asakura Hospital, Ishii Surgery Clinic, Shigematsu Medical Office, Tanabe Medical Office, Haki Clinic, Fukuoka Prefectural Hepato-gastroenterological Center, Moriyama Medical Office, Yamaga Medical Office, Wada Surgery Clinic, Chikugo River Onsen Hospital, Harazuru Onsen Hospital, Digestive Tract Internal Medicine of St. Mary's Hospital, Digestive Tract Internal Medicine of Koga Hospital, and Majima Digestive Tract Clinic. Moreover, we thank the following companies for supplying the related inspection reagent kits for the hepatitis virus: Ortho-Clinical Diagnostics, K.K., Roche Diagnostics K.K., and Abbott Laboratories. This study was supported in part by grants as a project for establishing new high technology research centers, by a Grant-in-Aid for Scientific Research (C) (No. 11670548), by a Grant-in-Aid for Encouragement of Young Scientists (No. 14770256) from the Ministry of Education, Science, Sports and Culture of Japan, and the Hepatitis C Research Group (2001-2003) under the auspices of the Ministry of Health, Labor and Welfare.

References

1. Maynard JE: Hepatitis B: global importance and need for control. Vaccine (Suppl): S18-S20, 1990.
2. WHO: Global surveillance and control of hepatitis C. Report of a WHO consultation organized in collaboration with the viral hepatitis prevention board, Antwerp, Belgium. J Viral Hepat 6: 35-47, 1999.
3. Niederau C, Lange S, Heintges T, *et al*: Prognosis of chronic hepatitis C: result of a large, prospective cohort study. Hepatology 28: 1687-1695, 1998.
4. Yoshizawa H: Hepatocellular carcinoma associated with hepatitis C virus infection in Japan: projection to other countries in the foreseeable future. Oncology 62 (Suppl 1): 8-17, 2002.
5. Yotsuyanagi H, Shintani Y, Moriya K, *et al*: Virologic analysis of non-B, non-C hepatocellular carcinoma in Japan: frequent involvement of hepatitis B virus. J Infect Dis 181: 1920-1928, 2000.
6. Pollicino T, Squadrito G, Cerenzia G, *et al*: Hepatitis B virus maintains its pro-oncogenic properties in the case of occult HBV infection. Gastroenterology 126: 102-110, 2004.
7. Blackberg J and Kidd-Ljunggren K: Occult hepatitis B virus after acute self-limited infection persisting for 30 years without sequence variation. J Hepatol 33: 992-997, 2000.
8. Fong T-L, Di Bisceglie AM, Gerber MA, *et al*: Persistence of hepatitis B. Hepatology 18: 1313-1318, 1993.
9. Kao JH, Chen PJ, Lai MY, *et al*: Occult hepatitis B virus infection and clinical outcomes of patients with chronic hepatitis C. J Clin Microbiol 40: 4068-4071, 2002.
10. Caccoiola I, PollicinoT, Squadrito G, *et al*: Occult hepatitis B virus infection in patient with chronic hepatitis C liver disease. N Engl Med 341: 22-26, 1999.
11. Sheu JC, Huang GT, Shin LN, *et al*: Hepatitis C and B viruses in hepatitis surface antigen-negative hepatocellular carcinoma. Gastroenterology 103: 1322-1327, 1992.
12. Paterlini P, Driss F, Nalpas B, *et al*: Persistence of hepatitis B and hepatitis C viral genomes in primary liver cancers from HBsAg-negative patients study of a low-endemic area. Hepatology 17: 20-29, 1993.
13. Kubo S, Nishiguchi S, Hirohashi K, *et al*: Clinical significance of prior hepatitis B virus infection in patients with chronic hepatitis C virus-related hepatocellular carcinoma. Cancer 86: 793-798, 1999.
14. Fukuda R, Ishimura N, Niigaki M, *et al*: Serologically silent hepatitis B virus confection in patients with chronic hepatitis C virus associated chronic liver disease: clinical and virological significance. J Med Virol 58: 201-207, 1999.
15. Uchida T, Kaneita Y, Gotoh K, *et al*: Hepatitis C virus is frequently coinfected with serum marker negative hepatitis B virus: probable replication promotion of the former by the latter as demonstrated by *in vitro* cotransfection. J Med Virol 52: 399-405, 1997.
16. Gonzalez S, Navas S, madejon A, *et al*: Hepatitis B and D genomes in hepatitis B surface antigen negative patients with chronic hepatitis C. J Med Virol 45: 168-173, 1995.
17. Villa E, Crottola A, Buttafoco P, *et al*: Evidence of hepatitis B virus in patients with chronic hepatitis C with or without serological markers of hepatitis B. Dig Dis Sci 40: 8-13, 1995.
18. Berger A, Doerr HW, Rabenau HF, *et al*: High frequency of HCV infection in individuals with isolated antibody to hepatitis B core antigen. Intervirology 43: 71-76, 2000.
19. Dickson RC, Everhart JE, Lake JR, *et al*: Transmission of hepatitis B by transplantation of livers from donors positive for antibody to hepatitis B core antigen. Gastroenterology 113: 1668-1674, 1997.
20. Uemoto S, Sugiyama K, Marusawa H, *et al*: Transmission of hepatitis B virus from hepatitis B core antibody-positive donors in living related liver transplants. Transplantation 65: 494-499, 1998.
21. Sagnelli E, Coppola N, Scolastico C, *et al*: HCV genotype and 'silent' HBV co-infection: two main risk factors for a more severe liver disease. J Med Virol 64: 350-355, 2001.
22. Joller-Jemelka J, Wicki A and Grob P: Detection of HBs antigen in anti-HBc alone positive sera. J Hepatol 21: 269-272, 1994.
23. Marusawa H, Umemoto S, Higikata, *et al*: Latent hepatitis B virus infection in healthy with antibodies to hepatitis B core antigen. Hepatology 31: 488-495, 2000.
24. Chiba T, Matsuzaki Y, Abei M, *et al*: Multivariate analysis of risk factors for hepatocellular carcinoma in patients with hepatitis C virus-related liver cirrhosis. J Gastroenterol 31: 552-558, 1996.
25. Okada S, Sato T, Okusaka T, *et al*: Past exposure to hepatitis B virus as a risk factor for hepatocellular carcinoma in patients with chronic liver disease. Br J Cancer 77: 2028-2031, 1998.
26. Marusawa H, Osaki Y, Kimura T, *et al*: High prevalence of anti-hepatitis B virus serological markers in patients with hepatitis C virus related liver disease in Japan. Gut 45: 284-288, 1999.

27. Sata M, Nakano H, Suzuki H, *et al*: Sero-epidemilogic study of hepatitis C virus infection in Fukuoka, Japan. J Gastroenterol 33: 218-222, 1998.
28. Nagao Y, Fukuizumi K, Tanaka K, *et al*: The prognosis for life in an HCV hyperendemic area. Gastroenterology 125: 628-629, 2003.
29. Okamoto H, Okada S, Sugiyama Y, *et al*: Detection of hepatitis C virus RNA by a two-stage polymerase chain reaction with two pairs of primers deduced from the 5'-noncoding region. Jpn J Exp Med 60: 215-222, 1990.
30. Nagao Y, Tanaka K, Kobayashi K, *et al*: Analysis of approach to therapy for chronic liver disease in an HCV hyperendemic area of Japan. Hepatol Res 28: 30-35, 2004.
31. Nagao Y, Tanaka K, Kobayashi K, *et al*: A cohort study of chronic liver disease in an HCV hyperendemic area of Japan: a prospective analysis for 12 years. Int J Mol Med 13: 257-265, 2004.
32. Feitelson MA and Duan LX: Hepatitis B virus X antigen in the pathogenesis of chronic infections and development of hepatocellular carcinoma. Am J Pathol 150: 1141-1157, 1997.
33. Tamori A, Nishiguchi S, Kubo S, *et al*: Possible contribution to hepatocarcinogenesis of X transcript hepatitis B virus in Japanese patients with hepatitis C virus. Hepatology 29: 1429-1434, 1999.
34. Zhou YZ, Slagle BL, Donehower LA, *et al*: Structural analysis of a hepatitis B virus genome integrated into chromosome 17p of a human hepatocellular carcinoma. J Virol 62: 4224-4231, 1988.
35. Khristova M, Nainan O, Xia G-L, *et al*: False-positive HBVDNA results among persons with only antibody to hepatitis B core antigen. Antiviral Ther 5 (Suppl 1): B22, 2000.
36. Ke-Qin H: Occult hepatitis B virus infection and its clinical implications. J Viral Hepat 9: 243-257, 2002.
37. Torbenson and Thomas DL: Occult hepatitis B. Lancet Infect Dis 2: 479-486, 2002.
38. Ide T, Kumashiro R, Koga Y, *et al*: A real-time quantitative polymerase chain reaction method for hepatitis B virus in patients with chronic hepatitis B treated with lamivudine. Am J Gastroenterol 98: 2048-2051, 2003.
39. Yano Y, Yamashita F, Sumie S, *et al*: Clinical significance of antibody against hepatitis B virus core antigen in patients infected with hepatitis C virus-related hepatocellular carcinoma. Liver Int 23: 227-231, 2003.
40. Hiraoka T, Katayama K, Tanaka J, *et al*: Lack of epidemiological evidence for a role of resolved hepatitis B virus infection in hepatocarcinogenesis in patients infected with hepatitis C virus in Japan. Intervirology 46: 171-176, 2003.
41. Matsuzaki Y, Chiba T, Hadama T, *et al*: HBV genome integration and genetic instabillity in HBsAg-negative and anti-HCV-positive hepatocellular carcinoma in Japan. Cancer Lett 119: 53-61, 1997.
42. Matsuzaki Y, Sato M, Saito Y, *et al*: The role of previous infection of hepatitis B virus in HBs antigen negative and anti-HCV-positive Japanese patients with hepatocellular carcinoma: etiological and molecular biological study. J Exp Clin Cancer Res 158: 73-84, 1999.
43. Chen P-J and Chen D-S: Hepatitis B virus infection and hepatocellular carcinoma. Molecular genetics and clinical perspectives. Semin Liver Dis 19: 253-262, 1999.

Luteolin Promotes Degradation in Signal Transducer and Activator of Transcription 3 in Human Hepatoma Cells: An Implication for the Antitumor Potential of Flavonoids

Karuppaiyah Selvendiran,[1] Hironori Koga,[1,2] Takato Ueno,[1,2] Takafumi Yoshida,[1,2] Michiko Maeyama,[1,2] Takuji Torimura,[1,2] Hirohisa Yano,[3] Masamichi Kojiro,[3] and Michio Sata[1,2]

[1]Research Center for Innovative Cancer Therapy, and Center of the 21st Century Center of Excellence Program for Medical Science, Kurume University; and [2]Second Department of Medicine and [3]Department of Pathology, Kurume University School of Medicine, Kurume, Japan

Abstract

In this study, we have investigated the underlying molecular mechanism for the potent proapoptotic effect of luteolin on human hepatoma cells both *in vitro* and *in vivo*, focusing on the signal transducer and activator of transcription 3 (STAT3)/Fas signaling. A clear apoptosis was found in the luteolin-treated HLF hepatoma cells in a time- and dosage-dependent manner. In concert with the caspase-8 activation by luteolin, an enhanced expression in functional Fas/CD95 was identified. Consistent with the increased Fas/CD95 expression, a drastic decrease in the Tyr^{705} phosphorylation of STAT3, a known negative regulator of Fas/CD95 transcription, was found within 20 minutes in the luteolin-treated cells, leading to down-regulation in the target gene products of STAT3, such as cyclin D1, survivin, Bcl-xL, and vascular endothelial growth factor. Of interest, the rapid down-regulation in STAT3 was consistent with an accelerated ubiquitin-dependent degradation in the Tyr^{705}-phosphorylated STAT3, but not the Ser^{727}-phosphorylated one, another regulator of STAT3 activity. The expression level of Ser^{727}-phosphorylated STAT3 was gradually decreased by the luteolin treatment, followed by a fast and clear down-regulation in the active forms of CDK5, which can phosphorylate STAT3 at Ser^{727}. An overexpression in STAT3 led to resistance to luteolin, suggesting that STAT3 was a critical target of luteolin. In nude mice with xenografted tumors using HAK-1B hepatoma cells, luteolin significantly inhibited the growth of the tumors in a dosage-dependent manner. These data suggested that luteolin targeted STAT3 through dual pathways—the ubiquitin-dependent degradation in Tyr^{705}-phosphorylated STAT3 and the gradual down-regulation in Ser^{727}-phosphorylated STAT3 through inactivation of CDK5, thereby triggering apoptosis via up-regulation in Fas/CD95. (Cancer Res 2006; 66(9): 4826-34)

Introduction

Flavonoids are polyphenolic compounds occurring naturally in the plant kingdom, displaying a wide range of pharmacologic properties, including anti-inflammatory, anticarcinogenic, and anticancer effects (1). Luteolin, the flavone subclass of flavonoids, usually occurs in its glycosylated form in celery, green pepper, perilla leaf, and camomile tea, etc., and much as an aglycone in perilla seeds. Recently, a potent anticancer effect of luteolin has been shown in several experiments *in vitro*; however, the bioavailability of luteolin has not yet been fully tested. Only one study on mouse skin cancer development has shown an anticancer effect of the luteolin-containing perilla leaf extract *in vivo* (2), suggesting a potential anticancer effect of any form of luteolin *in vivo*.

Apoptosis is supposed to be the main mechanism of the anticancer effects of luteolin, although other mechanisms, such as cell cycle inhibition by inactivating cyclin-dependent kinase 2 (CDK2; ref. 3), and antiangiogenesis by inhibiting vascular endothelial growth factor (VEGF)–induced phosphatidylinositol 3′-kinase activity (4), have been shown. The suggested mechanisms for the luteolin-induced apoptosis include activation of wild-type p53 (5), inactivation of receptor tyrosine kinase (6, 7), inactivation of topoisomerases (8, 9), sensitization to tumor necrosis factor-α (TNF-α; ref. 10), imbalance in Bcl-2 family of proteins (11–13), and inhibition of fatty acid synthase activity (14).

Signal transducer and activator of transcription 3 (STAT3) is a key signaling molecule for many cytokines and growth factor receptors (15). In addition, STAT3 is constitutively activated in a number of human tumors and possesses oncogenic potential and antiapoptotic activities (16–18). STAT3 is activated by phosphorylation at the Tyr^{705} residue, which induces dimerization, nuclear translocation, and DNA binding (19). Transcriptional activation seems to also be regulated by phosphorylation at the Ser^{727} residue, apparently via mitogen-activated protein kinase or via a mammalian target of rapamycin pathways (20, 21). Recently, the oncogenic transcription factor STAT3 has attracted much attention as a pharmacologic target, although *in vivo* evidence suggesting that inhibiting STAT3 could counteract cancer has remained incomplete (22).

CDK5 plays an essential role in both the development of the central nervous system during mammalian embryogenesis and maintenance of the neuronal architecture in the adult. Its deregulation has been implicated in neurodegenerative diseases (23). Although CDK5 binds to cyclins D and E, the activation of CDK5 requires one of its regulatory subunits, p35 or p39 (23). The extraneuronal expression of CDK5/p35 has been identified (24); however, the functional roles of CDK5 in the extraneuronal cells, such as liver cancer cells, have not yet been fully examined. Recently, CDK5 has been shown to regulate the phosphorylation of STAT3 on the Ser^{727} residue (25), suggesting that CDK5

Requests for reprints: Hironori Koga, Second Department of Medicine, Kurume University School of Medicine, 67 Asahi-machi, Kurume 830-0011, Japan. Phone: 81-942-31-7561; Fax: 81-942-34-2623; E-mail: hirokoga@med.kurume-u.ac.jp.

doi:10.1158/0008-5472.CAN-05-4062

participated in the oncogenic process through regulation of the STAT3 activity in neoplastic cells.

The aims of the present study were to clarify the detailed apoptotic mechanism of luteolin in human hepatoma cells *in vitro* and to assess the antitumor potential of luteolin *in vivo*. Here, we show a novel mechanism for luteolin-induced apoptosis to promote Tyr^{705}-phosphorylated STAT3 degradation. This unique mechanism of luteolin may lay the basis for the potent anticancer effect of luteolin, because STAT3 regulates expressions of crucial tumor-promoting gene products, including cyclin D1, survivin, Bcl-xL, and VEGF. We also show the luteolin-induced activation of Fas/CD95–mediated apoptosis through attenuation in the STAT3 expression. The *in vivo* antitumor effect of luteolin against hepatoma cell xenografts in nude mice suggests the bioavailability of this flavonoid.

Materials and Methods

Materials. Luteolin was isolated from perilla seeds and purified using high-performance liquid chromatography (purity >95%; Oryza Oil and Fat Chemical, Ichinomiya, Japan). Apigenin and (−)-epigallocatechin-3-gallate were purchased from Wako Pure Chemical Industries (Osaka, Japan). Recombinant human IFN-γ and recombinant human interleukin (IL)-6 were obtained from PeproTech (Rocky Hill, NJ). Antibodies against poly(ADP)ribose polymerase (PARP); Bcl-xL; survivin; phosphorylated STAT1; Tyr^{705}-phosphorylated STAT3; caspase-3; and cleaved caspase-3, caspase-7, and caspase-8 were purchased from Cell Signaling Technology (Beverly, MA). Anti-Fas/CD95 antibodies were from BD Biosciences (Franklin Lakes, NJ; clone DX2), and MBL (Nagoya, Japan; clone CH-11), respectively. Antibodies against glyceraldehyde-3-phosphate dehydrogenase (GAPDH), TNF receptor 1 (TNFR1), Fas/CD95 ligand, STAT1, STAT3, Ser^{727}-phosphorylated STAT3, STAT5, VEGF, ubiquitin, cyclin D1, CDK5, Tyr-phosphorylated CDK5, Ser-phosphorylated CDK5, and p35 were from Santa Cruz Biotechnology (Santa Cruz, CA). Antibodies against actin and FLAG were from Sigma (St. Louis, Missouri). MG-132, ALLN, roscovitine, and Ubiquitinated Protein Enrichment kit were from Calbiochem (San Diego, CA), and recombinant protein G agarose and the Lipofectamine kit were from Invitrogen (Carlsbad, CA). The caspase inhibitor Z-VAD-FMK was from Promega Corporation (Madison, WI). Enhanced chemiluminescence (ECL) reagents were obtained from Amersham Pharmacia Biotech (Buckinghamshire, United Kingdom), and the protein assay reagents were from Bio-Rad (Hercules, CA). The RNeasy kit was purchased from Qiagen (Valencia, CA). All other reagents and compounds were analytic grades.

Cell lines and cultures. Three human hepatoma cell lines, HepG2, HLF, and HAK-1B, and the human neuroblastoma cell line IMR-32 were used in this study. HepG2 and HLF were obtained from the Cancer Cell Repository of Tohoku University (Sendai, Japan) and the Human Science Research Resources Bank (Sennan, Japan), respectively. IMR-32 was from RIKEN BioResource Center (Tsukuba, Japan). HAK-1B was established in the Department of Pathology at our university (26). This cell line was well characterized and has often been used for s.c. transplantation into nude mice (27). Each cell line was grown in DMEM (Sigma-Aldrich Japan, Tokyo, Japan) supplemented with 10% heat-inactivated (56C, 30 minutes) fetal

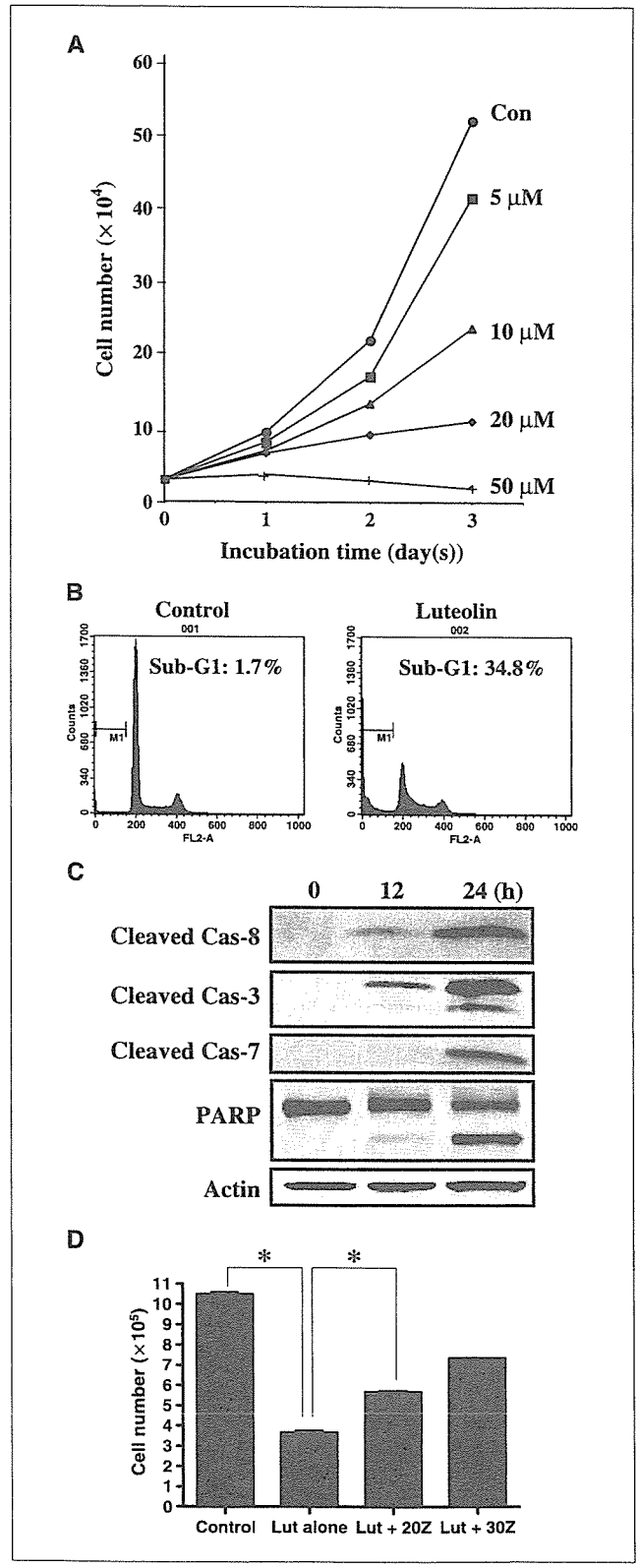

Figure 1. The proliferation-inhibitory effect of luteolin on HLF hepatoma cells. *A*, 2×10^4 HLF cells were seeded on a 60-mm-diameter dish, and incubated with each concentration of luteolin indicated up to 3 days. The cell number was counted at days 1, 2, and 3 after the seeding. Both a dosage- and a time-dependent inhibition of cell proliferation are shown. *B*, HLF cells were subjected to the 50 μmol/L luteolin treatment for 48 hours (*control*, vehicle-treated). Cells were then harvested, and the sub-G_1 population for 50,000 events within a fixed gate was analyzed. The indicated percentages are the mean of three independent experiments, each in duplicate. *C*, each sample of cell lysate containing of 50 μg protein was subjected to the immunoblot analysis for apoptosis. Cleavages in caspase-8, caspase-3, caspase-7, and PARP are clearly shown in the 50 μmol/L luteolin-treated HLF cells. *D*, 3×10^5 cells were seeded onto a 35-mm-diameter dish and cultured for 24 hours. Z-VAD-FMK or the vehicle (DMSO) was added to the medium at 1 hour before the 50 μmol/L luteolin treatment. After the 48-hour incubation, the attached cells were counted. *, $P < 0.001$; *Lut*, luteolin; *20Z*, 20 μmol/L Z-VAD-FMK; *30Z*, 30 μmol/L Z-VAD-FMK.

bovine serum (BioWest, Nuaill, France), 100 units/mL penicillin, and 100 μg/mL streptomycin (Invitrogen) in a humidified atmosphere of 5% CO_2 at 37C.

Cell counting. The cell numbers of both untreated and luteolin-treated HLF cells were counted using a CDA-500 automated cell counter (Sysmex, Kobe, Japan).

Cell cycle analysis by flow cytometry. The DNA content was assessed by staining ethanol-fixed cells with propidium iodide and monitoring by FACSCalibur (Becton Dickinson, Franklin Lakes, NJ). The percentage of cells in the sub-G_1 apoptotic cell population was determined using CELLQuest software (Becton Dickinson).

Immunoblot analysis. Hepatoma cells were lysed in lysis buffer [50 mmol/L Tris-HCl (pH 8.0), 150 mmol/L NaCl, 0.5% NP40, 1 mmol/L EDTA (pH 8.0), 1 mmol/L EGTA (pH 8.0), 0.1 mmol/L sodium fluoride (NaF), 0.1 mmol/L sodium orthovanadate (Na_3VO_4), 1 mmol/L DTT, 2 μg/mL aprotinin, and 2 μg/mL leupeptin]. Cell lysates were centrifuged at 12,000 × *g* for 20 minutes at 4°C, and the supernatant was separated. Xenografted tumor tissue samples were homogenized on ice in the lysis buffer, and the homogenate was clarified by centrifugation. The protein concentration was measured using a Bio-Rad protein assay kit. After being boiled for 5 minutes in the presence of 2-mercaptoethanol, samples containing cell or tissue lysate protein were separated on 10% or 15% SDS-polyacrylamide gel and then transferred onto equilibrated polyvinylidene difluoride membranes (Bio-Rad). After skimmed milk blocking, the membranes were incubated with the primary antibodies described above. The bound antibodies were detected with horseradish peroxidase (HRP)–labeled sheep anti-mouse IgG or HRP-labeled donkey anti-rabbit IgG (Amersham Pharmacia Biotech) using the enhanced chemiluminescence detection system (ECL Advanced kit). A positive signal from the target proteins was visualized using an image analyzer LAS-1000 plus (Fujifilm, Tokyo, Japan), and the fold increase and percentage reduction in the protein expressions were determined using an Image Gauge version 3.45 (Fujifilm).

Immunofluorescence confocal laser scanning microscopy. Immunocytochemistry was done as previously reported (28). Hepatoma cells, grown on Lab-Tek Chamber Slides (Nalge Nunc Int, Naperville, IL), were fixed with 4% paraformaldehyde for 10 minutes at room temperature, and then washed in PBS containing 0.05% Tween 20 (PBS-T). Nonspecific reactions were blocked with protein block serum-free (DAKO Japan, Kyoto, Japan) and then incubated with an anti-Tyr^{705}-phosphorylated STAT3 antibody at 4°C overnight. After washing in PBS-T, the specimens were treated with Alexa Fluor goat anti-mouse IgG (H+L) antibody (Molecular Probes, Eugene, OR) for 30 minutes at room temperature, and then counterstained by propidium iodide after digestion of RNA by RNase (Nippon Gene, Tokyo, Japan). A confocal laser scanning microscope (FLUOVIEW FV300; Olympus, Tokyo, Japan) equipped with an argon/krypton laser capable of dual excitation and detection was used to visualize the immunostaining for Tyr^{705}-phosphorylated STAT3 protein and the nuclear localization of propidium iodide. The negative stain control was done by omitting the primary antibody in the above experiment.

Reverse transcription-PCR. Total RNA was isolated from HLF cells using the RNeasy system according to the instructions of the manufacturer. RNA quantification was done using spectrophotometry. Reverse transcription-PCR (RT-PCR) analysis for the mRNA expressions in Fas/CD95 and the internal control GAPDH was carried out using a GeneAmp PCR System 9700 (Applied Biosystems, Foster City, CA), under the following conditions: initial denaturation at 94°C for 2 minutes, 35 cycles of amplification (denaturation at 94°C for 30 seconds, annealing at 50°C for 30 seconds, and extension at 72°C for 30 seconds), and extension at 72°C for 5 minutes. The sequences (5′-3′) for the primer pairs of Fas/CD95 and GAPDH, respectively, were as follows: Fas/CD95, CAAGGGATTGAAATTGAGGA (forward) and GACAAAGCCACCCCAAGTTA (reverse); GAPDH, GTCAACGGATTTGGTCGTATT (forward) and AGTCTTCTGGGTGGCAGTGAT (reverse). The PCR products were electrophoresed on 1.5% agarose gel, and stained with ethidium bromide.

Transfection of wild-type STAT3 cDNA. The STAT3 overexpression experiments were done using a wild-type STAT3 cDNA as previously described (29). The FLAG-tagged gene was transfected into HLF cells using the Lipofetamine kit according to the protocol of the manufacturer. At

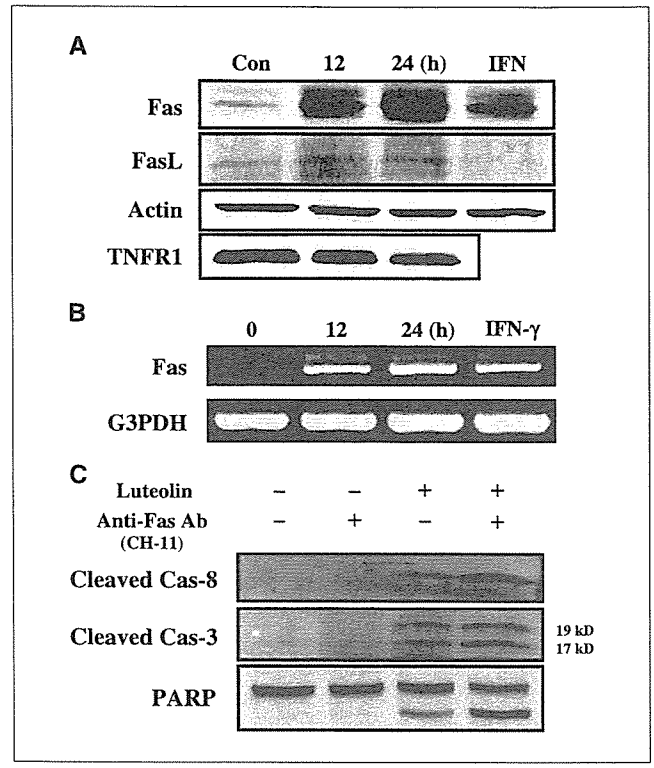

Figure 2. *A*, immunoblot analysis for the expression levels of caspase-8-associated death receptors, such as Fas/CD95 and TNFR1, and Fas/CD95 ligand (*FasL*). A clear increase in the Fas/CD95 expression, but not in the TNFR1 expression, is detected in the 50 μmol/L luteolin–treated HLF cells. The expression level of Fas/CD95 ligand is low and unchanged. *B*, the expression level of Fas/CD95 mRNA is increased in the 50 μmol/L luteolin–treated hepatoma cells. The IFN-γ (100 units/mL)–induced Fas/CD95 mRNA expression was set as a positive control. *C*, after incubation with 50 μmol/L luteolin for 12 hours, the agonistic anti-Fas/CD95 antibody (clone CH-11; dilution, 1:5,000) was added into the culture medium for the hepatoma cells. After treatment with the antibody for 4 hours, the cells were then prepared for immunoblot analyses of cleaved caspase-8, cleaved caspase-3, and PARP. The agonistic anti-Fas/CD95 antibody clearly increases the cleavages in caspase-8, caspase-3, and PARP, suggesting the enhanced apoptosis through stimulation of the newly synthesized Fas/CD95.

24 hours after the transfection of the *STAT3* gene, luteolin (50 μmol/L) was added into the culture medium of the cells, and the cells were subjected to immunoblots for Tyr^{705}-phosphorylated STAT3, total STAT3, cleaved caspase-3, PARP, and FLAG. The untransfected cells without the luteolin exposure, the untransfected cells with the luteolin exposure, the Lipofectamine-treated cell with the luteolin exposure, and the empty vector–transfected cells with the luteolin exposure were set as the controls.

Ubiquitination assay and immunoprecipitation. For the enrichment of any ubiquitinated proteins, affinity matrices consisting of a glutathione *S*-transferase fusion protein containing the ubiquitin-associated domains of Rad23 conjugated to glutathione-agarose (Ubiquitinated Protein Enrichment kit) were used. The affinity matrices were incubated with untreated or luteolin-treated HLF cell extracts (500 μg protein) in the lysis buffer for 2 hours. Then, the matrices were washed four times with the same buffer, and bound proteins were eluted with SDS loading buffer. The ubiquitinated protein-enriched samples were subjected to immunoblotting for ubiquitin, STAT3, Ser^{727}-phosphorylated STAT3, and Tyr^{705}-phosphorylated STAT3. Visualized smear signals were estimated as the polyubiquitinated target proteins. Immunoprecipitation was done as previously described (30) using an anti-STAT3 antibody for HLF cell lysates containing 200 μg protein.

Effects of luteolin on xenografted tumor growth in nude mice. Cultured HAK-1B (10^7 per mouse) was s.c. injected into the back of 5-week-old male BALB/c athymic nude mice (Clea Japan, Osaka, Japan). At 5 to

7 days later when the largest diameter of the tumor had reached ~5 to 8 mm, the mice were divided into three groups (n = 10 each) in a manner to equalize the mean tumor diameter among the three groups. Each mouse was given the CL-2 control diet, 50 or 200 ppm luteolin-containing CL-2-based diet (Clea Japan). The tumor size was measured in two orthogonal directions using calipers weekly, and the tumor volume (mm^3) was estimated using the equation length × $(width)^2$ × 0.5. At 6 weeks after the luteolin feeding, the mice were sacrificed and the tumors were resected. The tumor tissues were subjected to immunoblotting. All animal experiments were conducted in accordance with the NIH Guidelines for the Care and Use of Laboratory Animals and were approved by the University of Kurume Institutional Animal Care and Use Committee.

Statistical analysis. Statistical significance was assessed using Mann-Whitney U test. $P < 0.05$ was considered statistically significant.

Results

Luteolin inhibited cell proliferation, inducing apoptosis. Luteolin clearly inhibited proliferation in HLF cells in both dosage- and time-dependent manner. A 43.6% reduction in cell number was found in the luteolin-treated cells at a concentration of 10 μmol/L on day 3 (Fig. 1*A*). An induction in apoptosis contributed to this inhibition in cell proliferation (Fig. 1*B*). Moreover, 50 μmol/L luteolin showed a clear apoptosis in HLF cells within 12 hours, showing cleavages for caspase-8, caspase-3, caspase-7, and PARP in immunoblotting (Fig. 1*C*). Consistent with this finding, the caspase inhibitor Z-VAD-FMK significantly inhibited the luteolin-induced apoptosis in a dosage-dependent manner (Fig. 1*D*).

Involvement of Fas/CD95 in luteolin-induced apoptosis. Because caspase-8 was activated by luteolin, we examined the expression level of caspase-8-associated death receptors, such as Fas/CD95 and TNFR1. Indeed, a clear increase in Fas/CD95 expression, but not in TNFR1, was found in the luteolin-treated HLF cells (Fig. 2*A*), suggesting a significant involvement of Fas/CD95 in the luteolin-induced apoptosis. The expression level in the Fas/CD95 ligand in the luteolin-treated cells showed no change in comparison with that in the control cells (Fig. 2*A*), as recently reported in HepG2 cells (12). To confirm whether the increased expression in Fas/CD95 was due to its transcriptional induction, we did RT-PCR analysis for Fas/CD95 mRNA. The luteolin-treated HLF cells clearly showed an increased expression in Fas/CD95 mRNA (Fig. 2*B*). Then, we examined whether this up-regulated Fas/CD95 was functional in inducing apoptotic signals. We stimulated the luteolin-treated cells by an apoptosis-inducing anti-Fas/CD95 antibody (clone CH-11) and found that the pretreated cells became more sensitive to this antibody. This indicated that the newly synthesized Fas/CD95 was functional in mediating the apoptotic signals in the luteolin-treated human hepatoma cells (Fig. 2*C*).

Decrease in the expression level of phosphorylated STAT3s. Transcription of *Fas/CD95* is negatively regulated by STAT3, especially by its phosphorylated forms—Tyr^{705}-phosphorylated

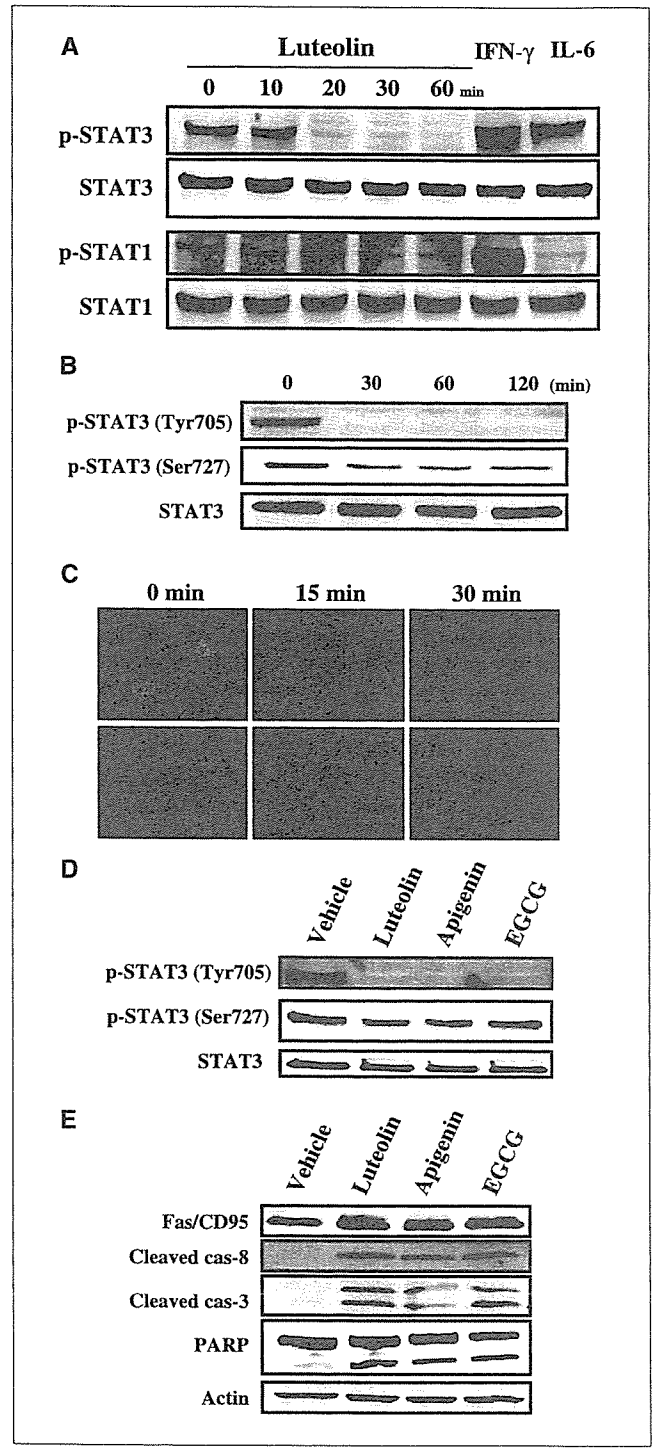

Figure 3. *A*, the time course study for the expression levels of STAT3 and STAT1 and their phosphorylated counterparts by immunoblot assay. The cells were treated with 50 μmol/L luteolin for 0, 10, 20, 30, and 60 minutes, respectively. For positive controls for Tyr^{705}-phosphorylated STAT3 (*p-STAT3*), HLF cells were incubated with IFN-γ (100 units/mL) and IL-6 (2 ng/mL). As for the positive control for phosphorylated STAT1 (*p-STAT1*), the IFN-γ-stimulated cells were used. The expression level of Tyr^{705}-phosphorylated STAT3 rapidly decreases after the 10-minute treatment of luteolin; however, that of phosphorylated STAT1 is unchanged by the luteolin treatment. *B*, a gradual decrease in the expression level of Ser^{727}-phosphorylated STAT3 [*p-STAT3 (Ser^{727})*] is noted in the luteolin-treated cells, compared with a marked decrease in that of Tyr^{705}-phosphorylated one [*p-STAT3 (Tyr^{705})*]. The total STAT3 expression level is almost unchanged. *C*, the active Tyr^{705}-phosphorylated STAT3 is confirmed to be in the nuclei of the hepatoma cells (*green signal*), and the expression of this type of STAT3 is diminished to an undetectable level within 30 minutes, which is consistent with the finding in the immunoblot analysis. *D*, other flavonoids, such as apigenin (25 μmol/L) and (−)-epigallocatechin-3-gallate (*EGCG*, 150 μmol/L), also show potential to decrease the expression level of Tyr^{705}-phosphorylated STAT3 to an undetectable level at 30 minutes after the treatments. *E*, the increase in the Fas/CD95 expression and the cleavages in caspase-8, caspase-3, and PARP are noted at 24 hours after the treatments with the flavonoids.

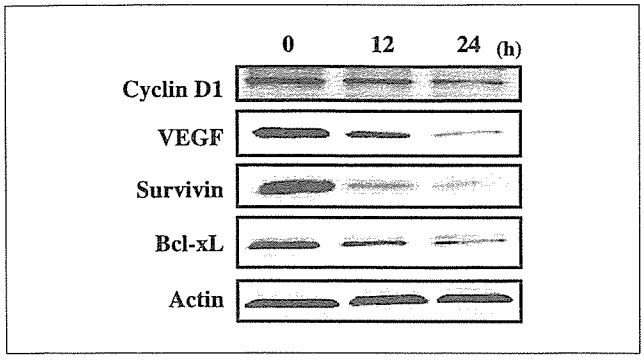

Figure 4. To assess the expression levels in the downstream gene products of STAT3, such as cyclin D1, VEGF, survivin, and Bcl-xL, the immunoblot analysis was done using the HLF cells exposed to 50 μmol/L luteolin for 12 and 24 hours. All of the gene products are found to be decreased in their expression levels by the luteolin treatment.

STAT3 and Ser^{727}-phosphorylated STAT3 (31). Thus, the increase in the expression level of Fas/CD95 by the luteolin treatment in this study encouraged us to investigate a possible decrease in the expression level of the phosphorylated STAT3s. And indeed, the expression level of Tyr^{705}-phosphorylated STAT3, a major phosphorylated STAT3, was drastically decreased within 20 minutes, although that of total STAT3 was mostly unchanged (Fig. 3*A*). In contrast to the rapid decrease in the Tyr^{705}-phosphorylated STAT3 expression level, a gradual decrease was found in the expression level of Ser^{727}-phosphorylated STAT3 (Fig. 3*B*). To ensure that this effect of luteolin was specific on the phosphorylated STAT3s, changes in the expression levels of phosphorylated STAT1 and phosphorylated STAT5 were examined using immunoblot analysis, resulting in no change in the phosphorylated STAT1 expression (Fig. 3*A*). STAT5 was barely expressed in the hepatoma cells used (data not shown). The drastic decrease in the nuclear Tyr^{705}-phosphorylated STAT3 was confirmed by immunocytochemistry using a confocal laser scanning microscope (Fig. 3*C*). Then, we assessed whether the specific decrease in the expression level of Tyr^{705}-phosphorylated STAT3 occurred universally in other flavonoids, including apigenin and (−)-epigallocatechin-3-gallate. These two flavonoids also decreased the expression of Tyr^{705}-phosphorylated STAT3 to an undetectable level at an early time point (within 30 minutes after treatment; Fig. 3*D*), followed by an increased expression of Fas/CD95 and the cleavages in caspase-8, caspase-3, and PARP at 24 hours after treatment (Fig. 3*E*).

Down-regulation in the STAT3 target genes. Because the oncogenic transcription factor STAT3 hierarchically up-regulates the tumorigenic genes, such as *cyclin D1, survivin, Bcl-xL*, and *VEGF* (15), we investigated the expression levels of the protein products of these genes by immunoblot assay. Indeed, all the gene products were clearly down-regulated (Fig. 4). Because these genes are involved in cell cycle progression (*cyclin D1*), antiapoptosis (*survivin* and *Bcl-xL*), and angiogenesis (*VEGF*), the down-regulation in these genes suggested a profound antitumor potential of luteolin even *in vivo*.

STAT3 overexpression leads to resistance to luteolin-induced apoptosis. If STAT3 was a critical target of luteolin, a profound expression of STAT3 should attenuate luteolin-induced apoptosis. To assess this hypothesis, we did a STAT3-overexpression experiment using cDNA of wild-type STAT3. The wild-type STAT3-overexpressing HLF cells showed an increased expression level in total STAT3, also generating a profound expression of both Tyr^{705}-phosphorylated STAT3 and Ser^{727}-phosphorylated STAT3. Despite luteolin treatment, the STAT3-overexpressing HLF cells had a clearly detectable level in the expression of Tyr^{705}-phosphorylated STAT3, which was fragile against luteolin in our system. As a result, the luteolin-treated STAT3-overexpressing cells showed no enhanced cleavages in caspase-3 or PARP, in

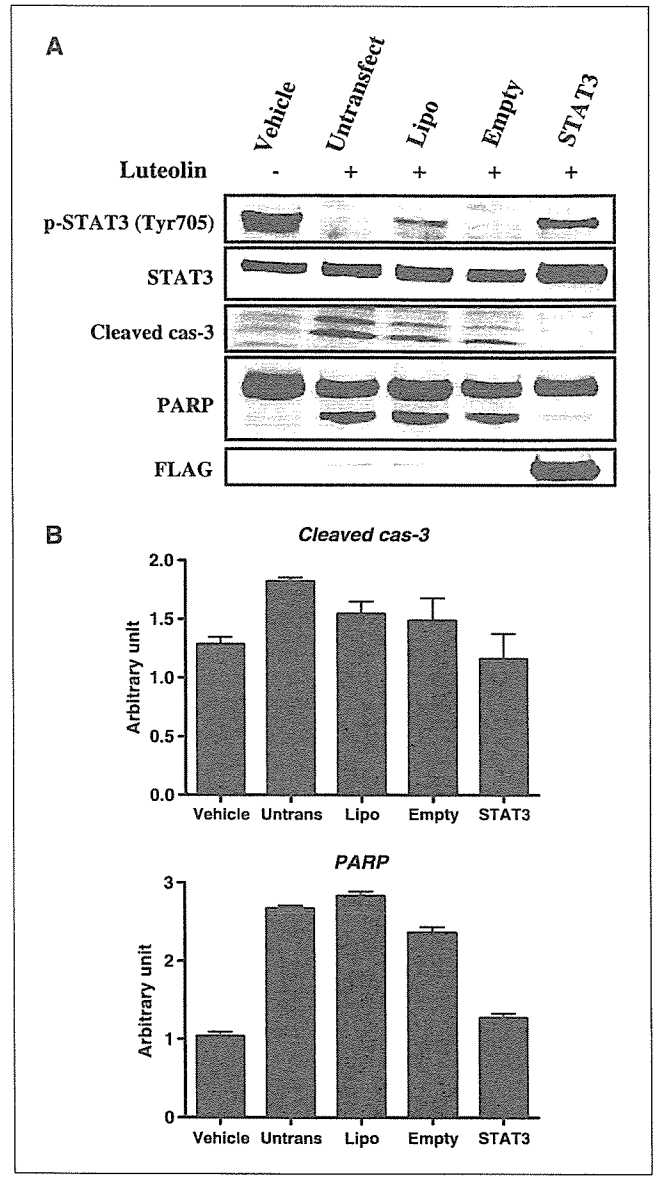

Figure 5. Resistance to the luteolin-induced apoptosis in the STAT3-overexpressing hepatoma cells. *A*, the *STAT3/FLAG* gene was transiently transfected into HLF cells by the lipofection method. At 24 hours after the transfection of the *STAT3* gene, luteolin (50 μmol/L) was added into the culture medium of the cells. The untransfected cells with vehicle (DMSO) alone, the untransfected cells with the luteolin exposure (*Untransfect*), the LipofectAMINE-treated cells with the luteolin exposure (*Lipo*), and the empty vector–transfected cells with the luteolin exposure (*Empty*) were set as controls. The *STAT3* gene–transfected HLF cells (*STAT3*) inhibit the luteolin-induced cleavages of both caspase-3 and PARP, showing an increased amount of total STAT3 and the detectable expression levels of Tyr^{705}-phosphorylated STAT3 and FLAG. *B*, densitometric analyses of visualized bands for cleaved caspase-3 and PARP. *Columns*, mean of three independent experiments; *bars*, SD.

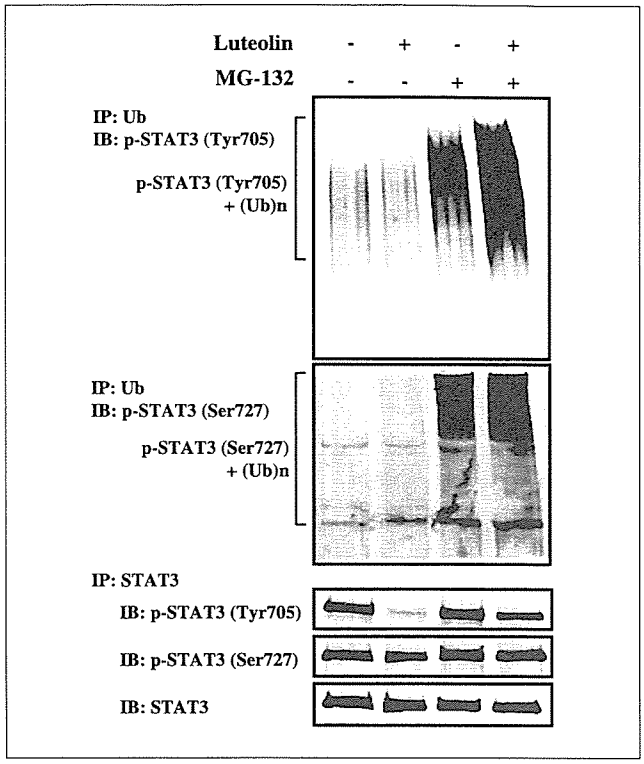

Figure 6. To catch any ubiquitinated proteins in the cell lysates, agarose beads coated with domains having affinity to ubiquitin were incubated in the lysates at 4°C for 2 hours. After washing the beads, the ubiquitinated proteins were subjected to immunoblot for Tyr^{705}-phosphorylated STAT3 and Ser^{727}-phosphorylated STAT3. A part of the lysate was also subjected to immunoprecipitation with anti-STAT3 antibody, and the immunoprecipitates were blotted by the antibodies for Tyr^{705}-phosphorylated STAT3, Ser^{727}-phosphorylated STAT3, and total STAT3. A predominant ubiquitination of the Tyr^{705}-phosphorylated STAT3 is seen in the luteolin-treated cells under proteasomal inhibition using MG-132 (50 μmol/L). In contrast, no clear increase in the ubiquitination of Ser^{727}-phosphorylated STAT3 is found by the luteolin treatment.

comparison with the controls including the empty vector–transfected cells (Fig. 5*A* and *B*), suggesting that luteolin might target, at least in part, STAT3 in the hepatoma cells.

Luteolin preferentially promotes ubiquitination of Tyr^{705}-phosphorylated STAT3. It is known that the intracellular amount of rapid-turnover proteins, including phosphorylated STAT3, is tightly regulated by the ubiquitin-dependent proteolytic pathway (30, 32, 33). In this study, a fast and marked decrease in the Tyr^{705}-phosphorylated STAT3 expression was found in the luteolin-treated cells, encouraging us to investigate any involvement of ubiquitin-dependent degradation in the drastic decrease in Tyr^{705}-phosphorylated STAT3 expression. Because HLF cells profoundly expressed the phosphorylated STAT3s, ubiquitination of the endogenous phosphorylated STAT3s was detected using the Ubiquitinated Protein Enrichment kit (Fig. 6). It was noteworthy that an enhanced polyubiquitination on Tyr^{705}-phosphorylated STAT3, but not on Ser^{727}-phosphorylated STAT3, was detected in the luteolin-treated cells, under the condition of coincubation with MG-132, a proteasome inhibitor (Fig. 6). This finding strongly suggested that luteolin ubiquitinated STAT3 in a phosphorylation site–specific manner in the human hepatoma cells.

Luteolin suppresses the expression level of tyrosine-phosphorylated CDK5. Recently, it has been shown that STAT3 is phosphorylated at a Ser^{727} residue by CDK5, a unique member of the CDK family (25). The activity of CDK5 is regulated by both formation of a complex with the partner molecule p35 (but not cyclins), and Tyr phosphorylation of CDK5 by a putative CDK5 kinase (23). Because we found a gradual decrease in Ser^{727}-phosphorylated STAT3, we investigated any possible earlier decrease in the p35 expression and/or the Tyr-phosphorylated CDK5 expression. To examine these expression levels, we set a positive control using the neuronal cell line, IMR-32, which has been shown to express a profound active CDK5 (34). HLF cells also expressed CDK5; however, its expression level was low in comparison with that of IMR cells. A clear decrease was identified in the expression level of Tyr-phosphorylated CDK5, but not in that of p35, in a luteolin dosage-dependent manner (Fig. 7*A*), suggesting less involvement of the p35 system in regulating Ser^{727} phosphorylation of STAT3 in the human hepatoma cells. In the time course experiments, the decrease in the expression level of Tyr-phosphorylated CDK5 was confirmed as an earlier event than the decrease in that of Ser^{727} phosphorylation of STAT3 (Fig. 7*B*). These findings suggested that luteolin predominantly decreased the expression level of Tyr-phosphorylated CDK5, thereby decreasing the expression level of Ser^{727}-phosphorylated STAT3, which was, at least in part, responsible for the attenuated activity of STAT3.

Inhibition in xenografted tumor growth by luteolin. Before going to animal experiments, we confirmed the potent apoptosis-inducing effect of luteolin in two other cell lines, HepG2 and HAK-1B. By the luteolin treatment, both HepG2 cells and HAK-1B cells clearly showed cleavages in caspase-3 and PARP, accompanied by decrease in the expression level of Tyr^{705}-phosphorylated STAT3 (Fig. 8*A*). Because HAK-1B cells were available for a xenograft

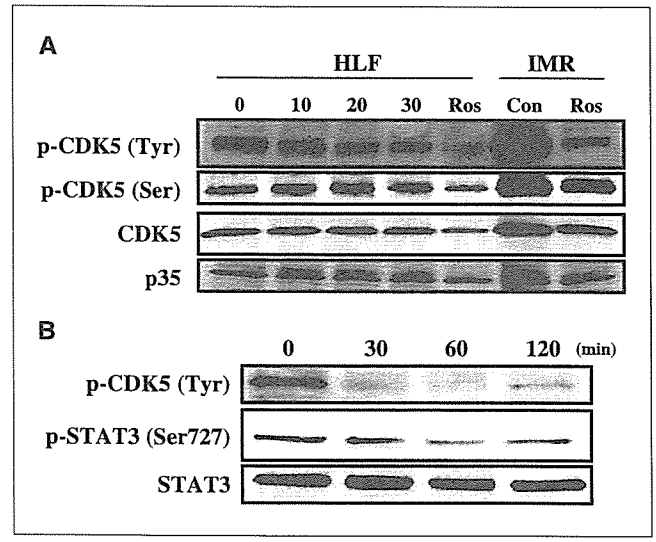

Figure 7. *A*, the hepatoma cells were incubated with 50 μmol/L luteolin for 0, 10, 20, and 30 minutes. A time-dependent decrease in the expression level of Tyr-phosphorylated CDK5 is noted in the immunoblot analyses. In contrast, the expression levels of Ser-phosphorylated CDK5 and p35 are unchanged by the luteolin treatments. The neuronal cell line IMR-32 (*IMR*) was set as the positive control for the active CDK5 expression. The expression levels of both Tyr-phosphorylated CDK5 and Ser-phosphorylated CDK5 are decreased by the CDK5 inhibitor, roscovitine (*Ros*, 10 μmol/L for 60 minutes incubation). *B*, a marked decrease in the expression level of Tyr-phosphorylated CDK5 is kept for at least 120 minutes by the 50 μmol/L luteolin treatment, followed by a gradual, but clear, decrease in that of Ser^{727}-phosphorylated STAT3.

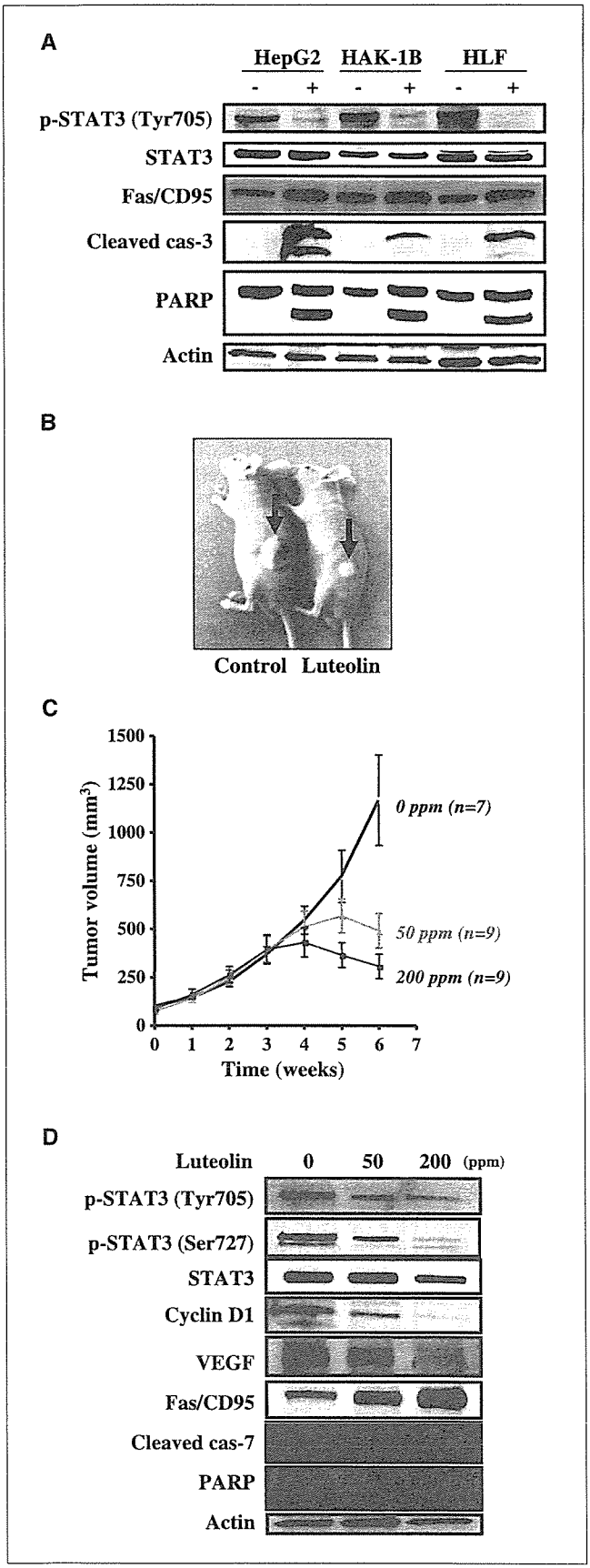

model in nude mice (27), the *in vivo* antitumor potential of luteolin was investigated (Fig. 8*B*). At 4 weeks after the beginning of luteolin-containing food intake, the HAK-1B tumor volume began to decrease in a dosage-dependent manner. After 5 weeks of the dietary luteolin treatment, a significant decrease in tumor volume was found even in mice taking 50 ppm luteolin-containing food (Fig. 8*C*). In concert with the decreased expressions in both Tyr^{705}-phosphorylated STAT3 and Ser^{727}-phosphorylated STAT3, a clear down-regulation in the target gene products of STAT3, such as cyclin D1 and VEGF, was found in the xenografted tumor tissues of the luteolin-treated mice, in a luteolin-dosage-dependent manner. Although an increased expression level of Fas/CD95 and a related cleavage in caspase-7 were confirmed in these tissue lysates, no clear cleavage was detected in PARP (Fig. 8*D*).

Discussion

In the present study, we have shown the following new findings: (*a*) luteolin increased the expression level of Fas/CD95 in neoplastic cells both *in vitro* and *in vivo*; (*b*) luteolin promoted the phosphorylation site–specific degradation in STAT3 through a ubiquitination-dependent process; and (*c*) luteolin significantly inhibited the growth in human hepatocellular carcinoma xenografts in nude mice.

Among several proposed mechanisms for the luteolin-induced apoptosis, the death receptor–associated mechanism has been recently receiving much attention. Shi et al. (10) first showed that luteolin sensitized TNF-α-induced apoptosis in malignant cells despite no significant increase in the TNFR1 expression level. Also, in our study, the expression level of TNFR1 was unchanged in the luteolin-treated hepatoma cells; however, a sensitization mechanism might underlie hepatoma cell apoptosis, presumably suppressing the expressions of the nuclear factor-κB (NF-κB)-targeted antiapoptotic genes (10). Very recently, it has been shown that luteolin up-regulated the death receptor 5 (DR5), thereby inducing apoptosis in human cancer cells and augmenting the apoptosis triggered by the DR5 ligand TNF-related apoptosis-inducing ligand (35, 36). These findings strongly suggested a critical involvement of the up-regulated death receptor superfamily–mediated signals in luteolin-induced cancer cell apoptosis. Also, in this study, up-regulation in another death receptor Fas/CD95 was first identified, even *in vivo*, in luteolin-treated human hepatoma cells, resulting in enhanced apoptosis via caspase-8 activation. It remains to be elucidated whether the death

Figure 8. *A*, a potent apoptosis-inducing effect of luteolin (50 μmol/L) is shown in three hepatoma cell lines. A marked decease in the expression level of Tyr^{705}-phosphorylated STAT3 accompanied by an increase in the Fas/CD95 expression is confirmed in all three cell lines, resulting in clear cleavages of caspase-3 and PARP in immunoblot assay. *B*, inhibition in the size of the xenografted HAK-1B tumors (*arrows*) is shown in a representative mouse taking the luteolin (200 ppm)–containing food. *C*, a clear decrease in the volume of the xenografted tumors is found. A dosage-dependent antitumor potential of luteolin is found *in vivo*. *D*, the tissue lysates of xenograft tumors, containing 50 μg protein each, were subjected to immunoblot analyses. The enhanced expression of Fas/CD95 is noted in the luteolin-exposed tumor lysates, in a dosage-dependent manner, in concert with the decreased expressions of both Tyr^{705}-phosphorylated STAT3 and Ser^{727}-phosphorylated STAT3. The decreased expressions are also shown in cyclin D1 and VEGF in a luteolin dosage–dependent manner. The cleavage of caspase-7 was found in the luteolin-exposed tumor lysates in a luteolin dosage–dependent manner; however, no clear cleavage was detected in PARP.

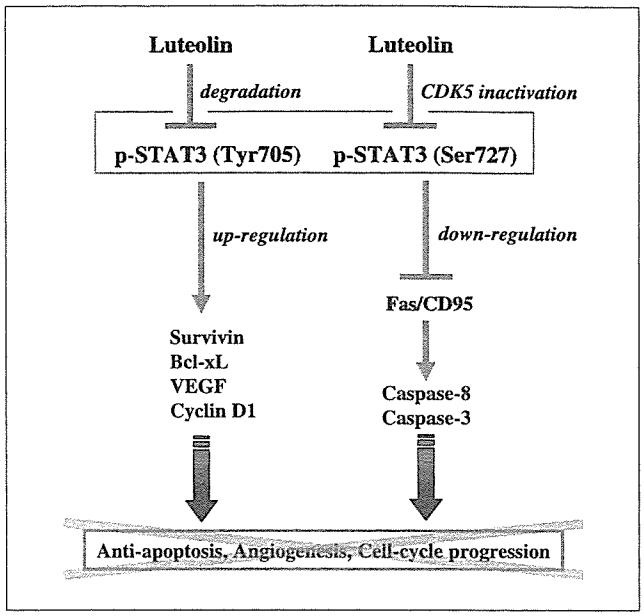

Figure 9. A schematic summary for the anticancer mechanisms of luteolin shown in the present study. Luteolin preferentially promotes the ubiquitin-dependent degradation in Tyr^{705}-phosphorylated STAT3, and participates, at least in part, in the down-regulation of Ser^{727}-phosphorylated STAT3 through inactivation of CDK5. This inactivation of STAT3 by luteolin may lead to the abrogation of the STAT3-mediated cancer properties, including antiapoptosis (survival), angiogenesis, and cell cycle progression, and increase sensitivity to apoptosis through up-regulation of Fas/CD95.

receptor–mediated apoptotic mechanism is ubiquitous in the flavonoid-induced apoptosis in malignant cells.

It has previously been shown that transcription of *Fas/CD95* was suppressed by the transcription factor, STAT3 (31). Because several up-regulated gene products by STAT3, such as cyclin D1, c-myc, Bcl-xL, survivin, and VEGF, are all critically involved in the development of cancer aggressiveness, targeting STAT3 is theoretically considered a fascinating anticancer strategy and has actually been shown to be valid in inducing a significant apoptosis in both the mice model of melanoma xenografts and that of squamous cell carcinoma xenografts (37, 38). Furthermore, ablation of STAT3 expression *in vivo* has provided a deep insight into a new candidate approach for the treatment of human lymphoma (39). In this context, our concerns converged in the potential effect of luteolin to down-regulate STAT3 expression as a putative mechanism for increased Fas/CD95 expression. Indeed, in this study, we found a drastic decrease in the expression level of Tyr^{705}-phosphorylated STAT3, a major active form of STAT3. Consistent with this finding in immunoblotting assay, we confirmed the immediate disappearance in Tyr^{705}-phosphorylated STAT3 from nuclei, where the activated STAT3 worked, in the luteolin-treated hepatoma cells by immunocytochemistry. If this striking down-regulation in active STAT3 is substantially responsible for the luteolin-induced apoptosis through augmenting Fas/CD95 expression, then enforced expression of STAT3 in hepatoma cells should result in luteolin resistance. Indeed, the transfected cells clearly expressed Tyr^{705}-phosphorylated STAT3 despite exposure to cytocidal concentrations of luteolin, resulting in less apoptosis. This finding strongly supports the concept that luteolin may induce apoptosis in human hepatoma cells by targeting the oncogenic transcription factor STAT3.

Although the precise mechanisms of STAT3 degradation have not yet been fully understood, it is evident that ubiquitination is involved in the proteasomal degradation of STAT3 (40–42). In the present study, we first showed an enhanced ubiquitination of Tyr^{705}-phosphorylated STAT3 by the natural flavonoid luteolin. This novel effect by luteolin may provide insights into the antitumor properties of natural agents. Recently, a mumps virus–derived protein has been shown to be involved in ubiquitin-dependent degradation in STAT3 (42); however, it still remains unclear whether such degradation is dependent on the phosphorylation status of STAT3. It is well known that many target proteins (substrates) for degradation are recognized by the substrate-specific E3 ligase [termed the Skp1/Cull 1/F-box (SCF)] complex, resulting in proteasomal degradation (43). Several substrates are captured by their corresponding E3-ligase complexes in a substrate phosphorylation–dependent manner. For example, SCF^{Skp2} targets phosphorylated forms of $p27^{Kip1}$ and p130. Thus, it is speculated that there may be a putative luteolin-(flavonoid)-responsive SCF machinery against Tyr^{705}-phosphorylated STAT3 in a phosphorylation-dependent manner.

STAT3 confers tumorigenic advantages to neoplastic cells through up-regulating cyclin D1, Bcl-xL, survivin, and VEGF (15). In the present study, the expression levels in all of these downstream molecules of STAT3 were clearly down-regulated by luteolin not only *in vitro* but also *in vivo*, even in mice ingesting a low concentration (50 ppm) of luteolin. It was suggested that these down-regulations contributed to the potent growth inhibitory effect on the xenografted cancers. In contrast, the clear increase in the Fas/CD95 expression by the luteolin-induced down-regulation of STAT3 seemed to contribute less to the significant apoptosis of xenografted hepatoma cells *in vivo*. It was noteworthy that the expression level of Ser^{727}-phosphorylated STAT3 was also clearly decreased. Because the Ser^{727} phosphorylation as well is known to regulate the transcriptional activity of STAT3 (20, 21), this attenuated phosphorylation was suggested to participate in the down-regulation of the transcriptional activity of STAT3 in the xenografted hepatoma cells in nude mice after long-term ingestion of luteolin. From our findings on the luteolin-induced dephosphorylation of CDK5, long-term exposure to luteolin *in vivo* might continuously inactivate CDK5, resulting in clear decrease in Ser^{727}-phosphorylated STAT3 expression.

Although the actual anticancer effects by luteolin both *in vitro* and *in vivo* are not yet agreed upon, the findings from the present study have suggested a dual-pathway theory targeting STAT3; one is the promotion of ubiquitin-dependent degradation in Tyr^{705}-phosphorylated STAT3 and the other is gradual down-regulation in Ser^{727}-phosphorylated STAT3 through inactivation of CDK5. These events on phosphorylated STAT3s (Fig. 9) may trigger apoptosis in cancer cells, although minimally *in vivo*, and/or inhibit cancer-promoting properties via up-regulation in Fas/CD95 and down-regulations in cyclin D1, Bcl-xL, survivin, and VEGF.

Acknowledgments

Received 11/16/2005; revised 2/13/2006; accepted 3/7/2006.

Grant support: Project grant for establishing new high technology research centers and grant from the 21st Century Centers of Excellence Program for Medical Science from the Ministry of Education, Culture, Sports, Science, and Technology of Japan.

The costs of publication of this article were defrayed in part by the payment of page charges. This article must therefore be hereby marked *advertisement* in accordance with 18 U.S.C. Section 1734 solely to indicate this fact.

We thank Masako Shinkawa for technical assistance.